Novel Bromodomain and extra-terminal (BET) protein inhibitor JQ1 sensitises Dexamethasone-resistant ALL cells to Dexamethasone-induced cell killing

By Joanna Longman

This project is submitted in partial fulfilment of the requirements for the award of the MRes

ACKNOWLEDGEMENTS

I would first like to thank my supervisor, Professor Tatjana Stankovic, for offering me the opportunity to carry out this research in her lab, and for her constant support, encouragement and enthusiasm throughout this project. I would also like to thank all other members of the Stankovic lab for their assistance, in particular Dr Tracey Perry for her invaluable support and endless patience.

Abstract

Background: B-cell precursor acute lymphoblastic leukaemia (ALL) is the most common paediatric malignancy. Proto-oncogene MYC functions as a DNA binding transcriptional activator. BET family proteins facilitate MYC transcription, and have recently emerged as a potential therapeutic target in heamopoitic malignancies. JQ1 is a cell-permeable small molecule that binds competitively to the acetyl-lysine recognition motifs with high specificity for the bromodomains of BET family members, preventing their ability to transcribe MYC. JQ1 inhibitor has previously demonstrated drastic anti-tumour activity *in vitro* and in pre-clinical models of c-Myc dependent malignancies

Aim: To investigate the sensitivity of ALL cells to JQ1-mediated BET inhibition, and whether JQ1 is capable of sensitising cytotoxic agent Dexamethasone resistant ALL cells to Dexamethasone induced cell killing both *in vitro* and *in vivo*.

Methods: Cytotoxicity assays were used to investigate JQ1-mediated Dexamethasone sensitisation in ALL cells *in vitro*. A Xenograft model was used to invesitagte this in NOG mice *in vivo*.

Results: JQ1-dexamethasone co-treatment resulted in significantly increased cell killing *in vitro* and complete tumour suppression *in vivo*.

Discussion: JQ1 is capable of sensitising Dexamethasone resistant ALL cells to Dexamethasone induced cell killing both *in vitro* and *in vivo*.

Contents

List of Figures

INDRODUCTION

1.1 B cells

B cells are an essential component of the humoral immune response [1]. They originate as immature stem cells in the bone marrow, which are then stimulated by cytokines and other chemical signals to migrate to the spleen and other secondary lymphoid tissues where they mature and differentiate into immunocompetent B cells [1, 2]. B cells secrete antibodies into the bloodstream to protect the body against foreign antigens and subsequent infection [2]. B cell activation is antigen-specific, and occurs by antigen recognition via B cell receptors (BCR). B cell activation also requires a secondary activation signal, usually provided by T-helper cells, another type of immune cell. This gives rise to B cell proliferation and B cell differentiation into antibody-secreting plasma cells [1].

1.2 B-cell precursor acute lymphoblastic leukaemia (ALL)

B-cell precursor acute lymphoblastic leukaemia (ALL) is an aggressive form of blood cancer in which early lymphoid precursor cells (B cell lymphoblasts) are arrested in an early stage of development [1]. This is caused by an abnormal expression of genes, often as a result of chromosomal translocations [1]. The lymphoblasts replace the normal marrow elements, resulting in a marked decrease in the production of normal blood cells. Consequently, anemia, thrombocytopenia, and neutropenia occur to varying degrees [3]. The lymphoblasts also proliferate in organs other than the marrow, particularly the liver, spleen, and lymph nodes [3].

Childhood cancers are generally rare. However, ALL is the most common paediatric malignancy, with approximately 500 cases diagnosed in children under 15 years old per year [4] . While ALL was incurable until the 1960's, mortality rates have improved significantly since [4]. The past two decades have seen dramatic increases in prognosis for ALL due to improved stratification of tumours and the rational use of intensive chemotherapy. As a result, paediatric ALL is now over

80% curable [5]. However, some patients still experience disease progression, suggesting a heterogeneous disease pathogenesis [3]. Further improvements in ALL treatment for such patients have remained elusive due to a lack of knowledge of basic molecular cancer cell biology and therefore targets to further individualise treatment. Some patients also suffer from long term, debilitating effects following chemotherapy due to its high toxicity and administration of large doses [6]. There is therefore a discernible need for more targeted treatment protocols. Treatments directed towards specific pathways involved in leukaemia pathology could dramatically improve the outcome for some patients [7].

1.3 Current chemotherapeutics

ALL cells exhibit a pathological increase in cell proliferation; a hallmark feature of virtually all cancer cells. A proportion of patient's exhibit defects in apoptosis in response to DNA damage. Such defects contribute to tumour progression, genetic instability and cytotoxic drug resistance [7].

The drugs commonly used as chemotherapeutics in ALL treatment are Vincristin, Daunorubicin, Cytosin arabinoside and Dexamethsone [8]. Dexamethasone is a glucocorticosteroid that induces apoptosis by downregulating pro-survival genes including Bcl-2 and Caspase activation with proven beneficial outcomes as a chemotherapeutic in various haemopoietic malignancies [8]. Glucocorticosteroids are currently the major component of therapeutic protocols for ALL, and sensitivity to them is still the most important prognostic parameter in ALL [9].

However, glucocorticosteroids including Dexamethasone are extremely cytotoxic to patients. Chronic nausea and neutropenia are common side effects of glucocorticosteroids [8]. Furthermore, due to the genetic instability and ability to undergo dysfunctional cell division, ALL cells are becoming increasingly resistant to current cytotoxic chemotherapeutics, including Dexamethasone [8]. This highlights the need for novel therapeutic agents targeting specific oncogenic pathways to become available for ALL patients.

1.4 The c-Myc oncogene

MYC is a well characterised proto-oncogene that encodes onco-protein c-Myc [5]. c-Myc functions as a DNA binding transcriptional activator, and is a critical regulatory factor of cell proliferation [10]. It binds to the local chromatin structure to activate transcription of certain genes [11, 12]. Amplification of MYC signalling is amongst the most common genetic alterations observed in cancer genomes, and has long been recognized as a key regulator of leukaemia biology [10]. Furthermore, up-regulation of MYC been suspected to play a role in the renewal of leukemic stem cells [13]. Constitutive over-expression of MYC contributes to pathogenesis of the majority of human cancers by co-ordinating the up-regulation of transcriptional programs influencing cell division and proliferation [10, 14]. Conditional transgenic models featuring tuneable transcriptional suppression have shown that even transient inactivation of MYC is capable of promoting tumour regression [15-18]. Numerous studies in various sub types of human leukaemia have validated c-Myc as an important therapeutic target [19-23].

However, the absence of a clear ligand binding domain means that a therapeutic approach to directly target the MYC gene has proven difficult [24-27]. Therefore, inhibition of MYC chromatin-dependent signal transduction provides an indirect means of targeting its transcriptional function [28]. MYC transcription is associated locally and globally with increased histone lysine side-chain acetylation; a covalent modification of chromatin that is regionally associated with transcriptional activation [29-31]. Histone acetylation templates the assembly of higher ordered transcriptional complexes by recruiting proteins with one or more acetyl-lysine-binding modules or bromodomains.

1.5 Bromodomain and extra-terminal (BET) proteins

The BET family of proteins are a subfamily of bromodomains that have recently emerged as a potential therapeutic target in heamopoietic malignancies [5]. The family includes proteins BRD2, BRD3, BRD4 and BRDT in humans. These BET proteins contain two conserved N-terminal

bromodomains (BRDs), small helical modules that specifically recognize acetylated lysine sites in proteins [32], an extra terminal domain (ET) and a more divergent C-terminal recruitment domain (CT motif or CTM) [33]. They associate with acetylated chromatin and facilitate transcription by increasing the effective molarity of recruited transcriptional activators [34]. They are key mediators for the assembly of the positive transcription elongation factor b complex (P-TEFb), an event required for the initiation of transcription elongation [35]. They bind to P-TEFb via their CT motif, tethering the complex to acetylated histone tails via their two N-terminal BRDs, resulting in assembly of the transcriptional machinery [35]. BRD4 in particular has been shown to remain bound to transcriptional start sites of genes expressed during mitosis and affects the transcription of growth and survival promoting genes [36]. It therefore marks select M/G1 genes in mitotic chromatin as transcriptional memory via direct interaction with the transcriptional elongation factor complex (pTEFb) [37]. Furthermore, a recent screen of an shRNA library targeting known epigenetic modifiers has identified BRD4 as the main factor that supports the maintenance of Acute Myloid Leukaemia (AML) stem cells [38]

The P-TEFb core complex is composed of cyclin-dependent kinase-9 (CDK9) and its activator cyclin T, and it functions to activate RNA polymerase II (RNAPol-II) [5]. The discovery that c-Myc regulates promoter-proximal pause release of pol II, also through the recruitment of P-TEFb [39] established a rationale for targeting BET bromodomains to inhibit c-Myc dependent transcription.

1.6 Novel pharmacological BET inhibitor JQ1

BET proteins were recently identified as the target of compound JQ1, molecular formula $C_{23}H_{25}ClN_4O_2S$. JQ1 is a cell-permeable small molecule that binds competitively to the acetyl-lysine recognition motifs with high specificity for the bromodomains of BET family members [40]. JQ1 binds to BRD4 bromodomains 1 and 2 with Kd values of ~ 50 and 90 nM, respectively [41]. This interaction prevents BET proteins from binding to acetylated chromatin and subsequent transcription facilitation [41].

JQ1 inhibitor has previously demonstrated anti-tumour activity *in vitro* and in pre-clinical models of c-Myc dependent malignancies. For example, Zuber et al showed that JQ1 treatment of numerous leukemic cell lines involving MLL and non-MLL translocations, primary leukemic cells, as well as mice bearing MLL-AF9/Nras G12D leukemic cells leads to leukemic cell death, myeloid differentiation and, in the case of the mice, extended survival[38]. It has also been demonstrated that it is possible to target the BET/histone interaction and directly inhibit it using the small molecule acetyl-lysine competitive inhibitor JQ1, resulting in epithelial differentiation, tumour shrinkage and survival in BRD4-NUT xenograft mice [40]. It therefore appears to be the case that BET inhibition by JQ1 results in cytotoxicity, the extent of which is determined by the disease phenotype of a particular haemopoietic malignancy.

It has been suggested that the main mechanism of JQ1 induced cytotoxicity involves downregulation of c-Myc and also of key anti-apoptotic protein Bcl-2 [42, 43]. While it has been proposed that ALL may well be another haemopoietic malignancy in which JQ1-mediated BET inhibition is therapeutically beneficial, the effect of JQ1 in ALL has yet to be defined, and a comprehensive study on ALL cell lines and primary ALLs bearing different features remains to be performed.

1.7 Aims and hypothesis

Dexamethasone is currently used as a chemotherapeutic for ALL treatment. However, high levels of toxicity and increasing drug resistance underpins the need for novel pharmacological treatments. When such a product becomes available, it is not usually administered in isolation, but in combination with other currently used therapeutics. The long term aim of this research is to optimise the clinical application of this promising potential novel therapeutic strategy. The aim of this study was therefore to investigate the sensitivity of ALL cells to JQ1-mediated BET inhibition, and whether JQ1 is capable of sensitising cytotoxic agent Dexamethasone resistant ALL cells to Dexamethasone induced cell killing both *in vitro* and *in vivo*. Furthermore, I aimed to expand upon

current understanding of JQ1s intracellular mechanism of BET inhibition. I analysed the sensitivity of an array of ALL cell lines harbouring various clinical and molecular features *in vitro*. I also explored the effect of JQ1-Dexamethasone co-treatment in Dexamethasone resistant ALL tumours in a xenograft model in NOG mice. I hypothesised that JQ1 would sensitise ALL cells to Dexamethasone both *in vitro* and *in vivo*.

2.0 MATERIALS AND METHODS

2.1 Materials

2.1.1 Cell lines and cell Culture

NALM-17 cell line was obtained by Dr. Yoshinobu Matsuo (Fujisaki Cell Center, Japan)

SD-1 cell line was obtained from DSMZ GmbH, Germany

REH cell line was obtained by Dr. Tony Ford (Institute of Cancer Research, Sutton, UK)

TOM-1 cell line was obtained from DSMZ GmbH, Germany

THP cell line was obtained from DSMZ GmbH, Germany

Table 1. Cell line information. Available information regarding cell lines used in this study. All cell lines were established from Leukaemia cells derived from patients diagnosed with ALL.

Cell line	Year established	Leukaemia type	Prognostic karyotype	Reference
Nalm-17	1978	Pre-β cell ALL	None	[44]
REH	1975	Common β cell ALL	Tel/AML 1	[45]
THP	1977	Pre-β cell AML	None	[46]
TOM1	1987	Pre-β cell ALL	BCR/ABL 1	[47]
SD1	1991	Pre-β cell ALL	BCR/ABL 1	[48]

2.1.2 Pharmaceuticals/chemical reagents

JQ1 10mM stock in DMSO - provided by Prof. Stefan Knapp (Structural Genomics Consortium, University of Oxford, UK)

Dexamethasone 10mM stock in DMSO – Sigma, UK

2.1.3 Buffers and solutions

RIPA lysis buffer – 1M tris-HlL pH7.4, sodium chloride, igepal, 1% sodium deoxycholate, 100mM EDTA and dH_2O

TBST – 1M tris-HCl pH7.6, 5mM sodium chloride, tween-80 and dH_2O

8% Resolving gel – 1.5M tris-HCl pH8.8, 40% polyacrylamide, 10% SDS, 10% APS, TEMED and dH_2O

5% Stacking gel – 0.8M tris-HCl pH6.8, 40% polyacrylamide, 10% SDS, 10% APS, TEMED and dH_2O

Gel sample buffer – 10% w/v DTT in laemlli buffer

10x Running buffer – tris base, glycine, SDS and dH_2O. Dilute to 1x in dH_2O

Transfer buffer – tris base, glycine, methanol, SDS and dH_2O

2.1.4 Additional materials

CellTiter-Glo Luminescent Cell Viability Assay – Promega, Southampton, UK

DL-Dithiothreitol (DTT) – Sigma, UK #D9779-10G

Phophate buffered saline (PBS) tablets – Sigma, UK #P4417-100TAB

Tween-80 – Sigma, UK #P4780

Methanol – VWR, UK #20847.307

Trypsin/EDTA – Invitrogen, UK #15400-054

Precision plus protein dual colour standards – Biorad, US #161-0374

Laemlli sample buffer – Biorad, US #161-0737

Amersham ECL plus western blotting detection system – GE life sciences, UK #RPN2132

TEMED – Sigma, UK #T9281

Sodium chloride – Fischer scientific, UK #S/3160/65

Medical X-ray film – Kodak, US #8143059

Sodium dodecyl sulphate (SDS) - Sigma, UK #L4390

Ammonium persulphate (APS) – Sigma, UK #A3678

Protease inhibitor cocktail – Sigma, UK #P8340

Amersham Hybond P PVDF membrane – GE life sciences, UK #RPN303F

2.2 Methods

2.2.1 Cell culture

All ALL cell lines were suspended in RPMI culture medium (Invitrogen, UK) supplemented with 10% foetal calf serum (Invitrogen, UK) and 1% penicillin/streptomycin antibiotics (Invitrogen, UK). Cells were maintained in 75 cm^3 vented cell culture flasks (Corning, UK), and incubated in humidified incubators at 37 °C, 5% CO_2. Cells were passaged every 7 days at a ratio of 1:10. The appropriate volume of cell suspension was transferred to fresh, pre-warmed media in a 75 cm^3 tissue culture flask.

2.2.2 Cell Viability Assays

The impact of JQ1 on cell viability was assessed in NALM-17, SD-1, TOM-1, THP and REH cell lines. Cell lines were seeded into opaque 96-well tissue culture treated plates at a density of $1x10^5$ cells/well in a volume of 195 µl of RPMI media. Cells were treated with or increasing concentrations of JQ1 (0.001 to 10 µM), with or without Dexamethasone. The desired concentration of the additional agent was added in a volume of 5 µl of media. Following incubation at 37 °C for 72 hours, the CellTiter-Glo Luminescent Cell Viability Assay (Promega Madison, WI) was used according to the manufacturer's instructions to indirectly evaluate the loss of cellular viability in response to drug treatment based on quantitation of the amount of ATP released by cells following lysis using the supplied reagents. Viability was measured on a Luminoskan Luminometer (Labsystems, Franklin, MA).

2.2.3 *In Vivo* xenograft study

All mouse experiments were approved by preclinical mouse models of leukaemias, ethical approval number RG-09-102. Animals were treated in accordance with UK Home Office guidelines, Schedule 1. NOG mice were obtained from Jackson labs at 6 weeks old, and were 9 weeks old when the experiment commenced. $5x10^6$ REH cells were transplanted by subcutaneous injection into the left flank per mouse. 4 weeks after injection, tumours became apparent. Mice then received one of four treatments; vehicle (10% cyclodextrin in PBS), Dexamethasone at 50 mg/Kg, JQ1 at 25 mg/Kg or Dexamethasone and JQ1 at 50 mg/Kg and 25 mg/Kg respectively (n=3 per group). Treatment was administered daily by intraperitoneal injection. Tumour burden in these models was quantified by caliper measurement.

2.2.4 Protein extraction

Mouse tumours from the *in vivo* xenograft experiment were harvested and lysed with 1 ml of RIPA lysis buffer. Whole cell lysates were then harvested and protein concentration was determined using Bicichoninic acid (BCA) assay using bovine serum albumin (BSA) as a standard. Lysates were

diluted to the appropriate concentration to give a constant protein concentration across samples. Samples were solubilised by laemlli buffer containing 10% DTT at 95 ^{0}C for 10 minutes and stored at -20 ^{0}C.

2.2.5 Western blot analysis

Mouse tumours from the previous *in vivo* experiment were harvested and lysed. SDS-PAGE was used for western blot analysis. Soluble protein samples were placed onto an 8% SDS-polyacrylamide gel alongside a molecular weight marker and electrophoresed at 140 V until the proteins were fully separated. Gels were then placed with a PVDF membrane in a blot cassette which was run for approximately 75 minutes at 360 mA to transfer proteins from the gel to the PVDF membrane. Membranes containing protein were then incubated at room temperature in 5% milk in TBST for 1 hour on an orbital rocker. Membranes were then incubated overnight with the following primary antibodies diluted in 5% milk in TBST at 4 ^{0}C: rabbit polyclonal against Mcl-1 (Santa Cruz Biotechnology), rabbit polyclonal against Survivin (Santa Cruz Biotechnology, UK), rabbit monoclonal against Parp-1 (Cell Signalling Technology, UK), mouse polyclonal against Bcl-2 (Sigma-Aldrich), rabbit polyclonal against IAP-2 (Sigma-Aldrich, US), and mouse monoclonal against β-actin for loading control (Sigma-Aldrich, US). All primary antibodies were used at 1:1000 dilutions. After washing 3 times with TBST for 10 minutes, the membranes were incubated with the appropriate horseradish peroxidase-conjugated secondary antibody diluted in 5% milk in TBST at room temperature for 1 hour. Secondary antibodies were used as follows: goat anti-rabbit polyclonal immunoglobulins + HRP at 1:3000 (Dako, US), goat anti-mouse polyclonal immunoglobulins + HRP at 1:1000 and 1:5000 for β-actin staining (Dako, US). Membranes were then washed again 3 times in TBST for 10 minutes and developed using ECL treatment and subsequent exposure on X-ray film, which was developed by the Xograph Compact X4 X-ray film processor.

2.2.6 Statistical analysis

Data are displayed as mean $\pm$ sem unless otherwise stated. Normally distributed data were statistically analysed using a two-tailed Student's *t*-test. A p value of <0.05 was considered to be statistically significant. All data analysis was carried out in Microsoft Excel 2010 version.

4. RESULTS

4.1 JQ1 sensitises ALL cells to Dexamethasone *in vitro* in some cell lines

I analysed loss of cell viability of five ALL cell lines following 72 hour incubation with increasing doses of JQ1 and Dexamethasone as single agents or in combination. Cell viability assays revealed that, in some cell lines, JQ1 sensitised ALL cells to Dexamethasone *in vitro* (Fig 1). Sensitisation was observed in Dexamethasone-resistant cell lines NALM-17 and REH. Dexamethasone treatment alone did not reduce the surviving fraction of cells in either cell line (Fig. 1a-b). JQ1 treatment alone at 0.1 μM also did not exhibit any apparent effect on the surviving fraction of cells in either cell line (Fig 1a-b). However, co-treatment of JQ1 and Dexamethasone did drastically reduce the fraction of surviving cells, suggesting that JQ1 and Dexamethasone acted synergistically even at the lowest doses. This highlights the potential for these two drugs to be used at doses which could reduce side effects of individual therapies of individual treatments.

There may also be some synergism between Dexamethasone and JQ1 in THP cells (Fig 1d), which appear to be insensitive to JQ1 treatment in isolation. However, JQ1 alone results in 41.09 $\pm$ 0.15 % of the cell population death, with only slightly more killing with JQ1 and Dexamethasone co-treatment. There also appears to be synergy between JQ1 and Dexamethasone in TOM-1 cells when Dexamethasone was used at 0.0001 μM and 0.001 μM. This effect became less prominent as the Dexamethasone concentration increased (Fig 1e). Dexamethasone treatment appears to result in the phenomenon of compensatory proliferation in NALM-17 cells (Fig 1a) [49, 50], where cellular stress due to the presence of a compound results in an initial compensatory increase in cell proliferation before the compound can induce cell death. The surviving fraction of cells also increases above 2 fold in SD1 cells treated with $\geq$ 0.1 μM. However, there does not appear to be a dose-response in this cell line and the s.e.m was much larger in SD1 cells treated with doses $\geq$ 0.1 μM Dexamethasone compared to other cell lines. I would therefore suggest that this experiment in SD1 cells was not technically accurate. A low level infection in SD1 cells or high

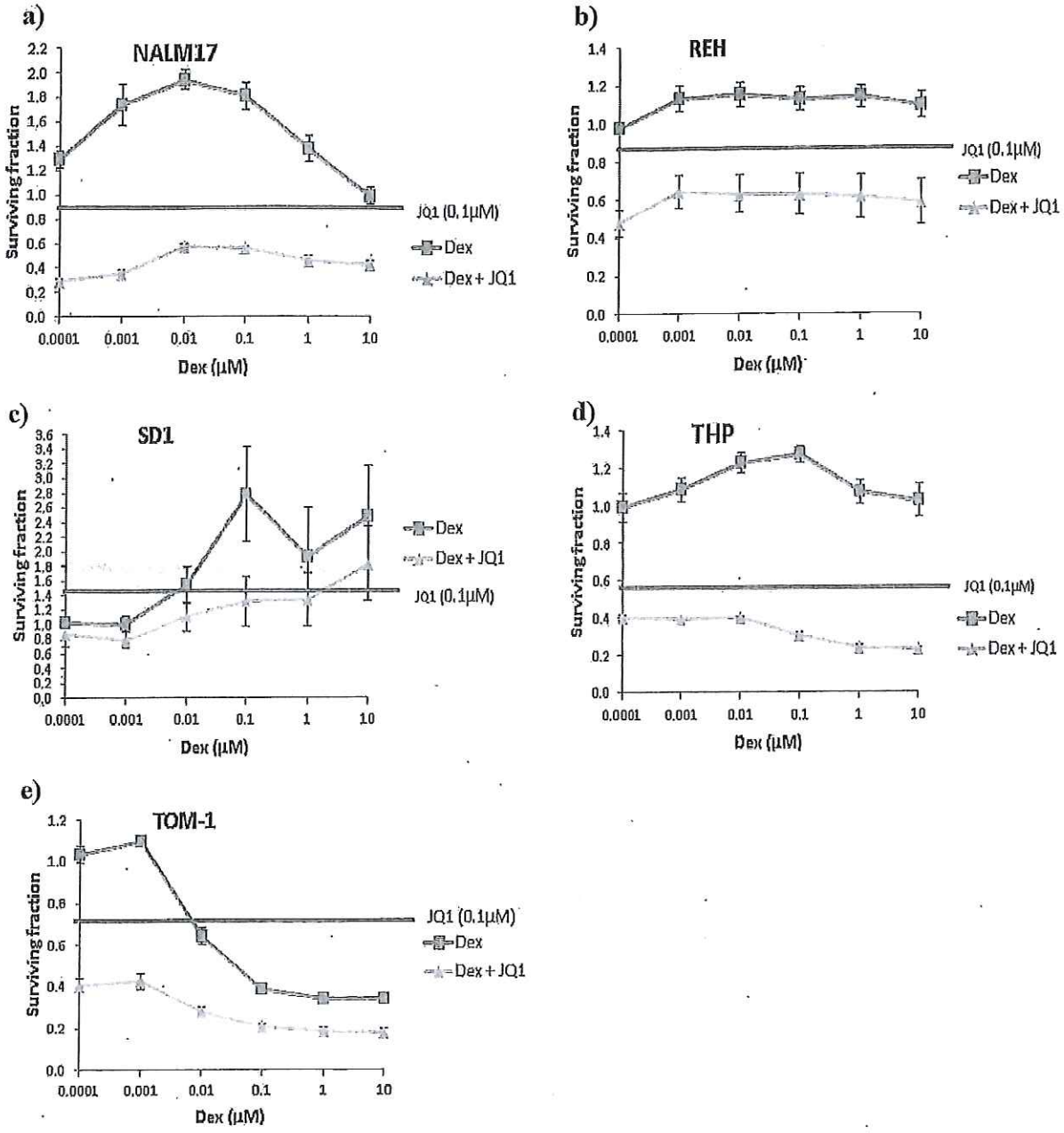

Fig 1. JQ1 sensitises ALL cells to Dexamethasone *in vitro*. ALL cell lines were incubated in triplicate with varying concentrations of dexamethasone (0.0001-10 μM, red line) 0.1μM JQ1 (blue line) or varying concentrations of dexamethasone (0.0001-10 μM) and 0.1μM JQ1in combination (green line) for 72 hours. Dexamethasone appears to result in the phenomenon of compensatory proliferation in NALM-17 cells. Data are presented at mean ± sem. Sensitisation to dexamethasone is evident in dexamethasone resistant cell lines NALM-17, REH and THP.

passage number could explain this result. Repetition of this experiment is SD1 cells would be required to reliably characterise the sensitivity or resistance of JQ1 and Dexamethasone treatment in this cell line.

4.2 JQ1 sensitises Dexamethasone-resistant cell line REH to Dexamethasone *in vivo*

To further investigate the effect of JQ1 on Dexamethasone antitumour efficacy, I explored a xenograft model of ALL. REH, a Dexamethasone-resistant ALL cell line, cells were injected by subcutaneous injection into NOG mice. After 4 weeks, tumours were apparent in 12 mice. These 12 mice were then administered one of four treatments; vehicle (PBS + 10% cyclodextrin [HPCD]), JQ1 (25 mg/kg), Dexamethasone (50 mg/kg) and JQ1 + Dexamethasone (25 mg/kg and 50 mg/kg respectively). Treatment was delivered by i.p injection three times weekly. Three mice were in each treatment group.

The recommended dose for *in* vivo experimental use of either JQ1 or Dexamethasone separately is 50 mg/kg [40, 51]. However, REH cells appear to be highly sensitive to JQ1 treatment, and only a small fraction of REH cells survive JQ1 treatment at higher doses (Fig 1). I wanted to test whether JQ1 treatment could sensitise Dexamethasone-resistant cell line REH to Dexamethasone treatment. I reasoned that administering the mice with a 50 mg/kg dose of JQ1 would be likely to result in REH tumour cell death regardless of the Dexamethasone treatment. I therefore treated the mice with a half dose (25 mg/kg) of JQ1 and a full dose of Dexamethasone (50 mg/kg).

The average tumour volume of mice that received JQ1 or Dexamethasone treatment did not significantly differ by day 10 from the mice that received the vehicle treatment over the course of the experiment (2717.00 mm^3, 2390.60 mm^3 and 2681.78 mm^3 respectively, $p>0.05$, Fig 2a). However, mice that received a combined treatment of JQ1 + Dexamethasone exhibited a

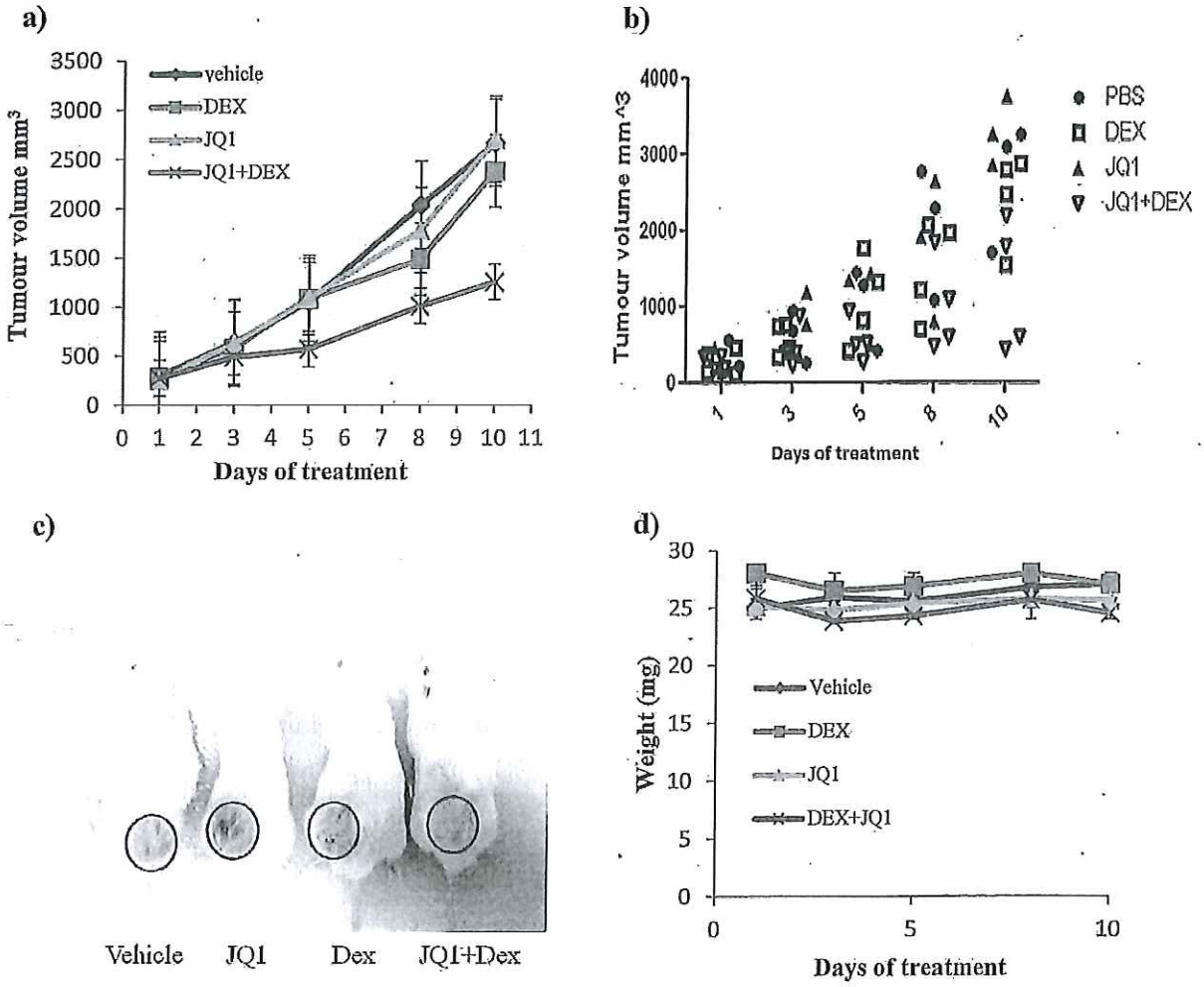

Fig 2. JQ1 and Dex combination therapy decreases tumour volume *in vivo*. a) Average tumour volume of NOG mice bearing REH subcutaneous tumours treated with vehicle (PBS + 10% cyclodextrin), JQ1 (25 mg/kg three times weekly, i.p), Dex (Dexamethasone) (10 mg/kg three times weekly, i.p), or JQ1 + Dex (25 mg/kg and 50 mg/kg respectively, three times weekly, i.p). Mice were given a total of 5 doses over 10 days. Statistical significance for difference in average tumour volumes compared to the vehicle was determined by paired, 2 tailed student's *t*-test. b) Scatter plot of NOG mice bearing REH subcutaneous tumours treated with vehicle, JQ1, Dex or JQ1 + Dex showing tumour volume of each mouse over the course of treatment. c) Photograph of tumour burdens of NOG mice bearing subcutaneous tumours. One representative mouse from each group (vehicle, JQ1, Dex, JQ1 + Dex) was photographed. Photograph was taken on day 10 after mice were sacrificed. d) Average weight of NOG mice bearing REH subcutaneous tumours for each treatment group (vehicle, JQ1, Dex, JQ1 + Dex). Statistical significance for difference in weight compared to the vehicle was calculated using paired, 2 tailed student's *t*-test.

significantly lower average tumour volume of 1258.46 mm^3 at day 10 than vehicle treatment ($p<0.05$). After this time, the average tumour volumes of the vehicle, JQ1 and Dexamethasone treatment groups exceeded 20,000 mm^3, which was deemed ethically unacceptable, and so the mice were sacrificed and the experiment terminated.

Due to the extremely small cohort of three mice per treatment group, the error bars in figure 2a are large and overlap. The range of tumour volumes within each treatment group therefore cannot be clearly seen. Figure 2b shows the tumour volume of each individual mouse over the course of treatment, and therefore the distribution of mice tumour volumes within each treatment group can be observed. Figure 2c displays photographic evidence of the decrease in tumour volume of JQ1 + Dexamethasone treated mice compared to the other three treatment groups. Figure 2 therefore indicates that JQ1 treatment of Dexamethasone treatment administered individually do not exhibit anti-tumour effects in REH tumours *in vivo*, but when administered together in a combination therapy, anti-tumour effects can be seen.

The average weights of the mice in each group did not significantly differ between groups or over the course of the experiment (Fig 2d, $p>0.05$ in all cases). This indicates that treatment was well tolerated and did not exhibit any other obvious adverse systemic effects.

4.3 JQ1 + Dexamethasone combined treatment may exhibit anti-tumour activity by inactivation of anti-apoptotic signalling pathways

NOG mice were sacrificed on day 10 of treatment because the average tumour volumes in vehicle, JQ1 and Dexamethasone treatment groups were greater than 20,000 mm^3. Tumours were then harvested and analysed for protein levels of key apoptosis regulators Mcl-1, Bcl-2, Survivin, Birc-3, and PARP-1 (Fig 3a). Details of the intracellular mechanism of apoptosis of each protein are listed in figure 3c. The β-actin loading control shows that unequal amounts of protein were loaded in each

a)

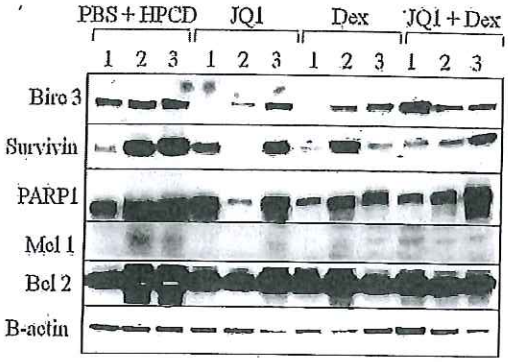

b)

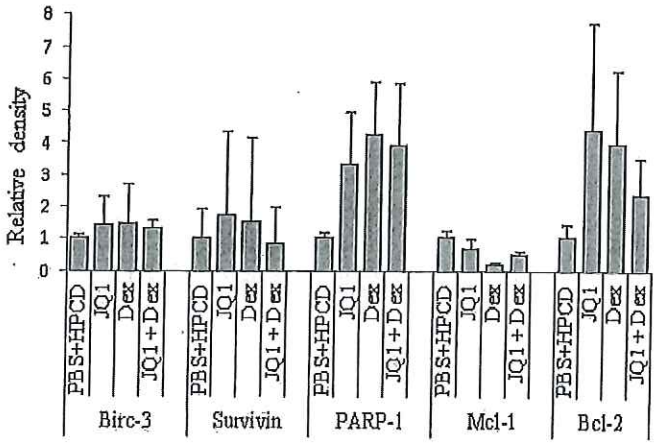

c)

Gene	Function
Birc-3	Inhibits apoptosis by binding to tumour necrosis factor receptor-associated factors TRAF1 and TRAF2, most likely by interfering with activation of ICE-like proteases
Survivin	Member of the inhibitor of apoptosis (IAP) gene family, which encode negative regulatory proteins that prevent apoptotic cell death. Expression is high in most tumour cells
PARP-1	Encodes a chromatin-associated enzyme, poly(ADP-ribosyl)transferase, which modifies various nuclear proteins by poly(ADP-ribosyl)ation. The modification is DNA-dependent and is involved in the regulation of various key cellular processes including differentiation, proliferation, tumour transformation and regulation of the molecular events involved in the recovery of cell from DNA damage
Mcl-1	Encodes an anti-apoptotic member of the Bcl-2 family. Enhances cell survival by inhibiting apoptosis
Bcl-2	Encodes an integral outer mitochondrial membrane protein that blocks the apoptotic death of some cells such as lymphocytes

Fig 3. Dexamethasone-JQ1 co-treatment may exhibit it's anti-tumour effect by downregulation of anti-apoptotic pathways. a) Profiling of in vivo response to JQ1, Dex or JQ1 + Dex combination in REH ALL Dex-resistant cell line by Western blotting. NOG mice subcutaneous tumours were harvested after the mice were sacrificed and analysed for protein levels of known apoptosis regulators. Each vertical lane represents a separate mouse. Each horizontal lane represents probing with a single antibody. These individual probings are separated by black boxes. JQ1 + Dex treatment shows decreased levels of Mcl 1, Bcl 2, Survivin, Birc 3, and PARP1 compared to the vehicle. B-actin staining was used as a loading control, although staining shows that protein loading was not equal between samples. b) Table detailing the functions of each gene encoding the proteins probed for in fig 3a.

case (Fig 3a). Therefore, interpretations as to whether protein levels of each apoptosis inhibitor have increased or decreased are difficult. Fig 3b shows the relative density of each blot compared to the β-actin loading control. The data are presented as fold change in protein levels compared to the average blot density of the vehicle treated mice. Fig 3b suggests that there may be an increase in PARP-1 and Bcl-2 protein levels in JQ1, Dexamethasone and JQ1+Dexamethasone treated mice compared to vehicle treated mice. There may also be a slight decrease in Mcl-1 protein levels in Dexamethasone and JQ1+Dexamethasone treated mice compared to vehicle treated mice. However, none of the differences in protein levels for any of the apoptosis regulators in any treatment condition compared to the vehicle treated mice was significant ($p>0.05$ in every case). This suggests that neither JQ1, Dexamethasone or JQ1+Dexamethasone treatment had a subsequent effect on any of the apoptosis inhibitors probed for in this study.

5. DISCUSSION

Debilitating side effects and increasing resistance to cytotoxic drugs such as Dexamethasone currently used in ALL clinical treatment highlights the need for novel therapeutic strategies of ALL. In this investigation, I have presented a new approach to ALL treatment which targets the histone acetyl-lysine binding bromodomains of BET proteins, which regulate transcriptional activation and epigenetic memory. This was demonstrated both *in vitro* and *in vivo*.

Firstly, I showed that BET inhibition with novel Bet protein inhibitor JQ1 sensitised Dexamethasone resistant cell lines NALM-17 and REH to Dexamethasone treatment *in vitro* (Fig 1a-b). JQ1 and Dexamethasone synergism can also be observed in TOM-1 cells when Dexamethasone is used at the lowest doses (0.0001 μM and 0.001 μM). Dexamethasone sensitivity remains a key predictor of prognosis, and many European pre-clinical trials include pre-treatment with glucocorticosteroids as an important stratification step [52-54]. However, Dexamethasone has been associated with severe and debilitating side effects due to the relative toxicity [8]. Methods to enhance the therapeutic efficacy of Dexamethasone even at low doses would therefore be of clinical interest [55].

I have shown sensitisation of Dexamethasone resistant cell lines with JQ1 treatment *in vitro* (Fig 1). In order to conclusively state that JQ1 does induce Dexamethasone sensitisation in Dexamethasone resistant ALL cell lines, I would have needed to have calculated the synergy between JQ1 and Dexamethasone in each cell line using Calcusyn software. However, due to time constraints this was not possible in this case. There also appeared to be a degree of JQ1-induced sensitisation to Dexamethasone in THP cells (Fig 1d). However, as these cells were fairly sensitive to JQ1-induced killing at 0.1 μM, only slightly more cell death was observed with JQ1 + Dexamethasone co-treatment. This is not necessarily detrimental in terms of potential clinical use of JQ1 + Dexamethasone combined treatment, but JQ1-induced sensitisation to Dexamethasone is difficult to analyse in THP cells due to their sensitivity to JQ1. In accordance with previous research [56] my

results show that TOM-1 cells are sensitive to Dexamethasone treatment in a dose-dependent manner (Fig 1e). Interestingly, JQ1 appears to sensitise TOM-1 cells to Dexamethasone at doses ≥ 0.01 μM. This finding has strong clinical implications, as Dexamethasone could be used at doses as low as 0.0001 μM in combination with JQ1 with similar efficacy as higher doses such as 1-10 μM.

Fig 2 shows that this sensitisation to Dexamethasone by JQ1 could also be induced *in vivo*. Combined treatment of JQ1 + Dexamethasone significantly decreased tumour volume compared to the vehicle treatment ($p<0.05$). Individual treatment of either Dexamethasone or JQ1 did not decrease tumour volume ($p> 0.05$ in both cases). Fig 3c shows the visible complete reduction of tumour size in mice that received Dexamethasone and JQ1 co-treatment compared to those that received vehicle, Dexamethasone or JQ1 treatment. Treatment was also well tolerated in all treatment conditions as represented by figure 3d. This has positive implications in terms of clinical applications at the used doses.

Taken together, these data prove that JQ1-mediated BET inhibition sensitises Dexamethasone resistant cells to Dexamethasone treatment. This JQ1-induced sensitisation to Dexamethasone could be because JQ1 downregulates multiple pro-survival genes that differ from glucocorticosteroid targets [57]. I therefore hypothesised that low/suboptimal doses of JQ1 would sensitise ALL cells to killing by Dexamethasone.

c-Myc is a well characterised proto-oncogene that functions as a DNA binding transcriptional activator, and is a critical regulatory factor of cell proliferation. Constitutive over-expression of c-Myc contributes to pathogenesis of the majority of human cancers by co-ordinating the up-regulation of transcriptional programs influencing cell division and proliferation [10, 14]. Transcriptional regulators BET proteins are involved in the chromatin-dependent signal transduction to RNA polymerase of c-Myc [40]. It has been suggested that the main mechanism of JQ1 induced cytotoxicity involves downregulation of MYC and also of key anti-apoptotic protein

Bcl-2 [58]. It is therefore likely that JQ1 acts by decreasing MYC transcription. This epigenetic modulation results in the subsequent decrease in MYC expression and therefore decreased tumourigenic activity. However, analysis of c-Myc protein levels and MYC expression would be needed to confirm this hypothesis.

Whilst c-Myc protein levels following JQ1, Dexamethasone or JQ1+Dexamethasone treatment in mice was not analysed in this study, I did measure protein levels for five known apoptosis inhibitors in mouse tumours following treatment in an attempt to identify specific anti-apoptotic pathways that JQ1+Dexamethasone co-treatment may downregulate to exhibit its antitumourigenic effect. However, Fig 3a-b revealed that there was no significant difference in protein levels of Birc-3, PARP-1, Mcl-1 or Bcl-2 ($p>0.05$ in all cases) under any treatment condition. This is most likely due to the fact that that standard error of the mean and therefore error bars are very large. This is because the sample cohort of only three mice per treatment group was extremely small. Furthermore, protein levels were analysed in mouse tumours, which inevitably more variable in terms of response to treatment than cell lines. This lack of difference may also be a consequence of tumour growth not being completely suppressed in a xenograft model by Dexamethasone or JQ1.

The *in vivo* part of this investigation in particular has strong clinical implications in terms of a novel combination therapy in which JQ1 is administered at small doses along with Dexamethasone to ALL patients to maximise the efficacy of Dexamethasone-mediated ALL cell killing. However, only three mice were in each treatment group. This extremely small cohort would first need to be broadened before accurate and valid conclusions about the optimal doses of JQ1 and Dexamethasone in co-treatment can be determined. Many more Dexamethasone resistant cell lines would need to be tested in a xenograft model such as this one. Primary ALL cells would also need to be investigated, since they better reflect the molecular environment of ALL patients.

In conclusion, my data suggest that BET inhibition is an effective novel target for paediatric ALL. I demonstrated that BET inhibitor JQ1 can sensitise ALL cells to current chemotherapeutic Dexamethasone at low doses, reducing cytotoxicity and debilitating side effects. My data also strongly supports the rationale for targeting BET proteins as a new therapeutic strategy that is able to enhance the efficacy of currently used strategies, therefore having a strong clinical significance.

6. FURTHER WORK

Future work should address whether the c-Myc is affected by JQ1-mediated BET inhibition in order to identify specific pathways involved in BET inhibition. Future studies should also address whether other chemotherapeutic with different mechanism of action can also be used in combination with JQ1 to provide a synergistic effect.

REFERENCES

1. *R&D Systems.* Research topics - B cells 01/05/2013]; Available from: http://www.rndsystems.com/molecule_group.aspx?g=694&r=1.
2. Disease, N.I.o.A.a.I. *Immune System.* 01/05/2013]; Available from: http://www.niaid.nih.gov/topics/immunesystem/immunecells/Pages/bcells.aspx.
3. Robison, L.L. and S. Bhatia, *Late-effects among survivors of leukaemia and lymphoma during childhood and adolescence.* British journal of haematology, 2003. **122**(3): p. 345-59.
4. *Children with cancer, UK.* Childhood Leukaemia 2012 01/05/2013]; Available from: http://www.childrenwithcancer.org.uk/childhood-leukaemia?gclid=CJHs68TU7bYCFc3HtAod1mEAaw.
5. Delmore, J.E., et al., *BET bromodomain inhibition as a therapeutic strategy to target c-Myc.* Cell, 2011. **146**(6): p. 904-17.
6. Bhatia, S., et al., *High risk of subsequent neoplasms continues with extended follow-up of childhood Hodgkin's disease: report from the Late Effects Study Group.* Journal of clinical oncology : official journal of the American Society of Clinical Oncology, 2003. **21**(23): p. 4386-94.
7. Weston, V.J., et al., *Apoptotic resistance to ionizing radiation in pediatric B-precursor acute lymphoblastic leukemia frequently involves increased NF-kappaB survival pathway signaling.* Blood, 2004. **104**(5): p. 1465-73.
8. Mitchell, C.D., et al., *Benefit of dexamethasone compared with prednisolone for childhood acute lymphoblastic leukaemia: results of the UK Medical Research Council ALL97 randomized trial.* British journal of haematology, 2005. **129**(6): p. 734-45.
9. Tissing, W.J., et al., *Molecular determinants of glucocorticoid sensitivity and resistance in acute lymphoblastic leukemia.* Leukemia, 2003. **17**(1): p. 17-25.
10. Dang, C.V., A. Le, and P. Gao, *MYC-induced cancer cell energy metabolism and therapeutic opportunities.* Clinical cancer research : an official journal of the American Association for Cancer Research, 2009. **15**(21): p. 6479-83.
11. Frank, S.R., et al., *Binding of c-Myc to chromatin mediates mitogen-induced acetylation of histone H4 and gene activation.* Genes & development, 2001. **15**(16): p. 2069-82.
12. Amati, B., et al., *Function of the c-Myc oncoprotein in chromatin remodeling and transcription.* Biochimica et biophysica acta, 2001. **1471**(3): p. M135-45.
13. Patel, J.H., et al., *The c-MYC oncoprotein is a substrate of the acetyltransferases hGCN5/PCAF and TIP60.* Molecular and cellular biology, 2004. **24**(24): p. 10826-34.
14. Kim, J., J.H. Lee, and V.R. Iyer, *Global identification of Myc target genes reveals its direct role in mitochondrial biogenesis and its E-box usage in vivo.* PloS one, 2008. **3**(3): p. e1798.
15. Jain, M., et al., *Sustained loss of a neoplastic phenotype by brief inactivation of MYC.* Science, 2002. **297**(5578): p. 102-4.
16. Soucek, L., et al., *Omomyc, a potential Myc dominant negative, enhances Myc-induced apoptosis.* Cancer research, 2002. **62**(12): p. 3507-10.
17. Soucek, L. and G. Evan, *Myc-Is this the oncogene from Hell?* Cancer cell, 2002. **1**(5): p. 406-8.
18. Soucek, L., et al., *Design and properties of a Myc derivative that efficiently homodimerizes.* Oncogene, 1998. **17**(19): p. 2463-72.
19. Gonda, T.J. and D. Metcalf, *Expression of myb, myc and fos proto-oncogenes during the differentiation of a murine myeloid leukaemia.* Nature, 1984. **310**(5974): p. 249-51.
20. Watt, R., et al., *Nucleotide sequence of cloned cDNA of human c-myc oncogene.* Nature, 1983. **303**(5919): p. 725-8.
21. Zhang, W., et al., *B-cell activating factor and v-Myc myelocytomatosis viral oncogene homolog (c-Myc) influence progression of chronic lymphocytic leukemia.* Proceedings of the National Academy of Sciences of the United States of America, 2010. **107**(44): p. 18956-60.
22. Rodig, S.J., et al., *The pre-B-cell receptor associated protein VpreB3 is a useful diagnostic marker for identifying c-MYC translocated lymphomas.* Haematologica, 2010. **95**(12): p. 2056-62.

23. Ott, C.J., et al., *BET bromodomain inhibition targets both c-Myc and IL7R in high-risk acute lymphoblastic leukemia.* Blood, 2012. **120**(14): p. 2843-52.
24. Amati, B., et al., *The c-Myc protein induces cell cycle progression and apoptosis through dimerization with Max.* The EMBO journal, 1993. **12**(13): p. 5083-7.
25. Blackwood, E.M. and R.N. Eisenman, *Max: a helix-loop-helix zipper protein that forms a sequence-specific DNA-binding complex with Myc.* Science, 1991. **251**(4998): p. 1211-7.
26. Blackwood, E.M., et al., *The Myc:Max protein complex and cell growth regulation.* Cold Spring Harbor symposia on quantitative biology, 1991. **56**: p. 109-17.
27. Darnell, J.E., Jr., *Transcription factors as targets for cancer therapy.* Nature reviews. Cancer, 2002. **2**(10): p. 740-9.
28. Schreiber, S.L. and B.E. Bernstein, *Signaling network model of chromatin.* Cell, 2002. **111**(6): p. 771-8.
29. Frank, S.R., et al., *MYC recruits the TIP60 histone acetyltransferase complex to chromatin.* EMBO reports, 2003. **4**(6): p. 575-80.
30. Fernandez, P.C., et al., *Genomic targets of the human c-Myc protein.* Genes & development, 2003. **17**(9): p. 1115-29.
31. Vervoorts, J., et al., *Stimulation of c-MYC transcriptional activity and acetylation by recruitment of the cofactor CBP.* EMBO reports, 2003. **4**(5): p. 484-90.
32. Muller, S., P. Filippakopoulos, and S. Knapp, *Bromodomains as therapeutic targets.* Expert reviews in molecular medicine, 2011. **13**: p. e29.
33. Medicine, N.D.o. *Structural Role of BET proteins in Transcription Initiation.* 2013 01/05/2013]; Available from: http://www.ndm.ox.ac.uk/doctoral-projects/project/structural-role-of-bet-proteins-in-transcription-initiation.
34. Rahman, S., et al., *The Brd4 extraterminal domain confers transcription activation independent of pTEFb by recruiting multiple proteins, including NSD3.* Molecular and cellular biology, 2011. **31**(13): p. 2641-52.
35. Bres, V., S.M. Yoh, and K.A. Jones, *The multi-tasking P-TEFb complex.* Current opinion in cell biology, 2008. **20**(3): p. 334-40.
36. He, N., et al., *Human Polymerase-Associated Factor complex (PAFc) connects the Super Elongation Complex (SEC) to RNA polymerase II on chromatin.* Proceedings of the National Academy of Sciences of the United States of America, 2011. **108**(36): p. E636-45.
37. Bisgrove, D.A., et al., *Conserved P-TEFb-interacting domain of BRD4 inhibits HIV transcription.* Proceedings of the National Academy of Sciences of the United States of America, 2007. **104**(34): p. 13690-5.
38. Zuber, J., et al., *RNAi screen identifies Brd4 as a therapeutic target in acute myeloid leukaemia.* Nature, 2011. **478**(7370): p. 524-8.
39. Rahl, P.B., et al., *c-Myc regulates transcriptional pause release.* Cell, 2010. **141**(3): p. 432-45.
40. Filippakopoulos, P., et al., *Selective inhibition of BET bromodomains.* Nature, 2010. **468**(7327): p. 1067-73.
41. BioVision. *Bromodomain inhibitor (+)-JQ1.* 2013 01/05/201

]; Available from: http://www.biovision.com/bromodomain-inhibitor-jq1-5584.html.
42. Holien, T., et al., *Addiction to c-MYC in multiple myeloma.* Blood, 2012. **120**(12): p. 2450-3.
43. Holien, T. and A. Sundan, *Oncogene addiction to c-MYC in myeloma cells.* Oncotarget, 2012. **3**(8): p. 739-40.
44. Matsuo, Y. and H.G. Drexler, *Establishment and characterization of human B cell precursor-leukemia cell lines.* Leukemia research, 1998. **22**(7): p. 567-79.
45. Rosenfeld, C., et al., *Phenotypic characterisation of a unique non-T, non-B acute lymphoblastic leukaemia cell line.* Nature, 1977. **267**(5614): p. 841-3.
46. Tsuchiya, S., et al., *Establishment and characterization of a human acute monocytic leukemia cell line (THP-1).* International journal of cancer. Journal international du cancer, 1980. **26**(2): p. 171-6.

47. Okabe, M., et al., *Establishment and characterization of a cell line, TOM-1, derived from a patient with Philadelphia chromosome-positive acute lymphocytic leukemia.* Blood, 1987. **69**(4): p. 990-8.
48. Dhut, S., et al., *Establishment of a lymphoblastoid cell line, SD-1, expressing the p190 bcr-abl chimaeric protein.* Leukemia, 1991. **5**(1): p. 49-55.
49. Mollereau, B., et al., *Compensatory proliferation and apoptosis-induced proliferation: a need for clarification.* Cell death and differentiation, 2013. **20**(1): p. 181.
50. Huang, Q., et al., *Caspase 3-mediated stimulation of tumor cell repopulation during cancer radiotherapy.* Nature medicine, 2011. **17**(7): p. 860-6.
51. Bradner, J.E. *Compound JQ1 user guide.*
52. Roy, A., et al., *Early response to induction is predictive of survival in childhood Philadelphia chromosome positive acute lymphoblastic leukaemia: results of the Medical Research Council ALL 97 trial.* British journal of haematology, 2005. **129**(1): p. 35-44.
53. Bostrom, B.C., et al., *Dexamethasone versus prednisone and daily oral versus weekly intravenous mercaptopurine for patients with standard-risk acute lymphoblastic leukemia: a report from the Children's Cancer Group.* Blood, 2003. **101**(10): p. 3809-17.
54. Mitchell, C., et al., *The impact of risk stratification by early bone-marrow response in childhood lymphoblastic leukaemia: results from the United Kingdom Medical Research Council trial ALL97 and ALL97/99.* British journal of haematology, 2009. **146**(4): p. 424-36.
55. Vrooman, L.M., et al., *Postinduction dexamethasone and individualized dosing of Escherichia Coli L-asparaginase each improve outcome of children and adolescents with newly diagnosed acute lymphoblastic leukemia: results from a randomized study--Dana-Farber Cancer Institute ALL Consortium Protocol 00-01.* Journal of clinical oncology : official journal of the American Society of Clinical Oncology, 2013. **31**(9): p. 1202-10.
56. Nehme, A. and J. Edelman, *Dexamethasone inhibits high glucose-, TNF-alpha-, and IL-1beta-induced secretion of inflammatory and angiogenic mediators from retinal microvascular pericytes.* Investigative ophthalmology & visual science, 2008. **49**(5): p. 2030-8.
57. Filippakopoulos, P., et al., *Benzodiazepines and benzotriazepines as protein interaction inhibitors targeting bromodomains of the BET family.* Bioorganic & medicinal chemistry, 2012. **20**(6): p. 1878-86.
58. Blobel, G.A., et al., *A reconfigured pattern of MLL occupancy within mitotic chromatin promotes rapid transcriptional reactivation following mitotic exit.* Molecular cell, 2009. **36**(6): p. 970-83.

Does microRNA deregulation contribute to PTTG1-Binding Factor (PBF) overexpression in thyroid carcinoma?

By Joanna Longman

This project is submitted in partial fulfilment of the requirements for the award of the MRes

ACKNOWLEDGEMENTS

I would first like to thank my supervisor, Professor Chris McCabe, for offering me the opportunity to carry out this research in his lab, and for his constant support throughout this project. I would also like to thank all other members of the McCabe lab for their assistance, in particular Dr Martin Read for this invaluable support and technical assistance.

Abstract

Background: Thyroid carcinomas are the most common malignancy of the endocrine system. The proto-oncogene PBF is upregulated in thyroid carcinoma. MicroRNAs (miRNAs) are small, endogenously expressed non-coding RNAs that negatively regulate target gene expression by mRNA degradation and/pr translational repression. They bind their target mRNAs by complementary base pairing to a region in the 3'UTR. miR-122 has recently been shown to regulate PBF expression.

Aim: To determine whether deregulation of miRNAs that target PBF drive PBF overexpression in thyroid carcinoma.

Methods: Computational miRNA target prediction was used to identify miRNAs that potentially target PBF. TaqMan PCR and Western blotting were used to analyse PBF expression following transfection with selected miRNA mimics.

Results: PBF expression was significantly decreased in TPC-1 cells transfected with mimics of miR-122-5p, miR-124a-3p and miR-506-3p.

Discussion: miR-122, miR-124 and miR-506 might target and be involved in the regulation of PBF, and may therefore contribute to the overexpression of PBF in thyroid carcinoma.

Contents

List of Figures

1. INTRODUCTION

1.1 The Thyroid Gland

The thyroid gland is a butterfly shaped endocrine organ (Fig 1) located in the neck, anterior to the larynx [1]. It consists of two lateral lobes connected by a narrow section called the isthmus [1]. Histological studies have identified three major components of the thyroid gland; thyroid follicles, thyroid follicular cells and parrafollicular C cells [1]. Thyroid follicles consist of a thyroid follicular cell monolayer which encompasses a colloid-filled cavity. This forms the major structural component of the thyroid. Parafollicular C cells also inhabit the monolayer and produce calcitonin [1].

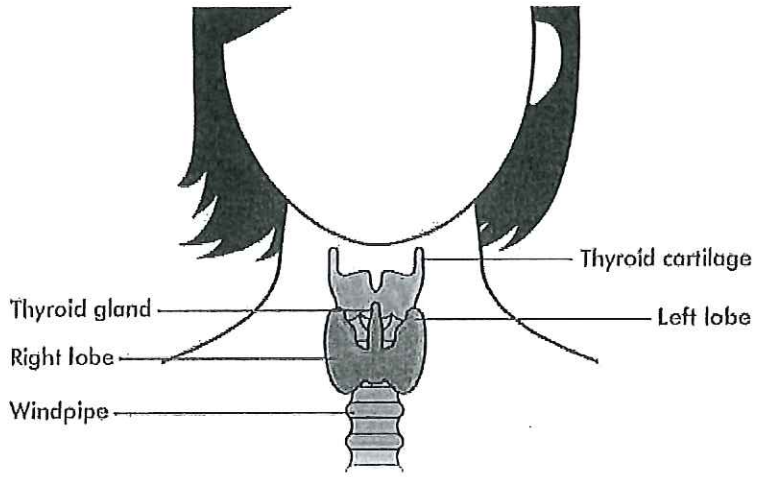

Figure 1. The thyroid gland. The thyroid gland is an organ located in the neck, anterior to the larynx. It is composed of two lateral lobes connected by an isthmus, creating it's characteristic butterfly shape.

Figure taken from Macmillan Cancer Support, The Thyroid Gland – Cancer information. Available at: http://www.macmillan.org.uk/Cancerinformation/Cancertypes?Thyroid/Aboutthyroidcancer/Thethyroidgland.aspx. Last updated01/04/2010

The main function of the thyroid gland is to synthesise and secrete thyroid hormones, primarily tetraiodothyronine (T_4) and 5,3,5'-triiodothyronine (T_3). Hormone synthesis occurs in the follicular cells and is iodine dependent [1].

1.2 Thyroid Carcinoma

Thyroid carcinomas are the most common malignancy of the endocrine system. They account for approximately 1% of all human cancers [2], and are becoming increasingly prevalent [3, 4]. In 2008, an estimated 213,000 cases of thyroid cancer were diagnosed worldwide [2]. However, their apparent increased incidence rate may be due to improved pathological detection and diagnosis [5]. Current treatment strategy is primarily total thyroidectomy, followed by post-operative 131I therapy [2]. While most differentiated thyroid carcinomas have a good prognosis, up to 35% recur, representing a need for effective diagnosis and therapeutics [3] [6].

Various subtypes of thyroid carcinoma display different histological characteristics, and can be categorised according to their cellular origin [7]. Carcinomas originating from thyroid follicular cells are typically differentiated carcinomas, or undifferentiated anaplastic thyroid carcinoma [7, 8]. Follicular (FTC) and papillary (PTC) thyroid carcinoma are characterised as differentiated carcinomas. FTC and PTC account for approximately 80% of all diagnosed thyroid carcinoma cases [3].

1.3 Mechanisms of thyroid cancer carcinogenesis

Due to their increasing incidence rate and relatively high risk of relapse, mechanisms of thyroid carcinogenesis and progression are currently of high interest amongst endocrinologists. Several

factors, both environmental and genetic, have been implicated in playing critical roles in thyroid cancer pathogenesis [9].

Genetic instability leads to increased acquisition of mutations and therefore increased tumour initiation and progression [10]. It is consequently causative factor in almost all human carcinomas [11]. In thyroid carcinoma, many proto-oncogenes and tumour suppressor genes appear to be deregulated [10]. For example, pathogenic activation of oncogenic intracellular signalling pathways including Wnt signalling and mitogen-activated protein kinase (MAPK), have been shown to contribute to thyroid cancer cell growth [12] [13], [14]. Furthermore, around 70% of PTCs have been shown to possess a nonoverlapping genetic alteration, either a BRAF or RAS mutation or RET/PTC rearrangement, resulting in the activation of MAPK signalling [7].

Understanding the genetic factors underlying thyroid carcinoma tumour initiation and growth is crucial to developing more effective stratification of tumours and treatment protocols. However, detailed molecular knowledge of the genetic and epigenetic events contributing to thyroid cancer carcinogenesis remains to be elucidated.

1.4 PTTG1-binding factor (PBF)

Pituitary tumour transforming gene (PTTG) has been identified as a proto-oncogene in many cancers. Its expression has also been highly correlated with thyroid cancer [15-17]. PTTG is a multifunctional protein that can transactivate basic fibroblast growth factor (FGF-2), an action that is dependent on PTTG-binding factor (PBF) [18].

PBF, also known as PTTG1IP or c21orf3 [19], is a poorly characterised protein. The PBF gene is located in the chromosomal region 21q22.3, and it encodes a protein of 180 amino acids with a predicted mass of 22KDa [18].Importantly, sequence analysis has revealed that the peptide

sequence is highly conserved across many animal species, indicating evolutionary importance and unique function [17]. PBF was initially thought to be a cell membrane glycoprotein until a bipartile nuclear localisation signal was observed, suggesting PBF may also be a nuclear protein.

Whilst structural and localisation studies with regards to PBF have been informative, comparatively little has been reported on its intracellular function. PBF has been shown to regulate cell cycle progression and separation of sister chromatids during mitosis [17]. PBF is overexpressed in some cancers, particularly in thyroid carcinomas, promoting transformation *in vitro* and is tumourigenic *in vivo* [17, 20, 21]. It may therefore promote tumour growth by pathologically driving cell cycle progression and replication. Furthermore, increased PBF expression in breast cancer has been shown to induce cell invasion, another hallmark of malignant carcinomas [20]. PBF therefore appears to have multiple roles within the cell and therefore numerous methods of promoting tumourigenesis. However, its exact function, role in carcinogenesis and mode of regulation is not known.

1.5 MicroRNAs

MicroRNAs (miRNAs) are small, endogenously expressed non-coding RNAs. miRNAs are generally located in the intergenic regions of the genome, approximately 1 kb away from predicted genes, although a minority are located in the intronic regions of known genes in the sense or antisense orientation [22], [23]. However, over 50% of miRNAs are found in close proximity to other miRNAs [24]. Analysis of miRNA gene expression showed that clustered miRNAs can be transcribed as polycistronic primary transcripts (pri-mRNAs), whereas those that are not in close proximity to other miRNAs are transcribed from their own promoters [25, 26].

miRNA transcription is thought to be carried out by RNA polymerase II [27] (Fig 2). miRNAs are transcribed as long primary transcripts that contain a local hairpin structure [27]. The stem-loop structure is then cleaved by RNase-III Drosha in the nucleus to create a precursor of miRNA (pre-miRNA) [27]. They are then exported into the cytoplasm where they are processed into mature miRNA duplexes by cytoplasmic RNase-III enzyme Dicer [28-31]. Mature miRNAs become incorporated into effector complexes known as miRNA-containing RNA-induced silencing complex (miRISC) [32].

MicroRNAs negatively regulate gene expression through the 3' untranslated region (3' UTR) of their target messenger RNA (mRNA) [33] [34] in a tissue specific manner [35-37]. This is achieved by mRNA degradation, where the miRNA acts as a guide molecule, directing the miRISC to the target mRNA site by complementary base pairing [38] [39]. Endonuclytic cleavage of the mRNA then occurs [40] and the mRNA fragment is degraded by major cellular -5' to -3' exonucleases [41]. However, it has also been shown that miRNAs can regulate gene expression via translational repression. This stemmed from earlier observations that some miRNAs, for example lin-14 miRNA, reduced protein levels without or with minimal effect on the amount of target mRNA [42, 43]. Recent studies suggest that miRISC complexes can repress translation by decreasing the rate of translation initiation [44-46].

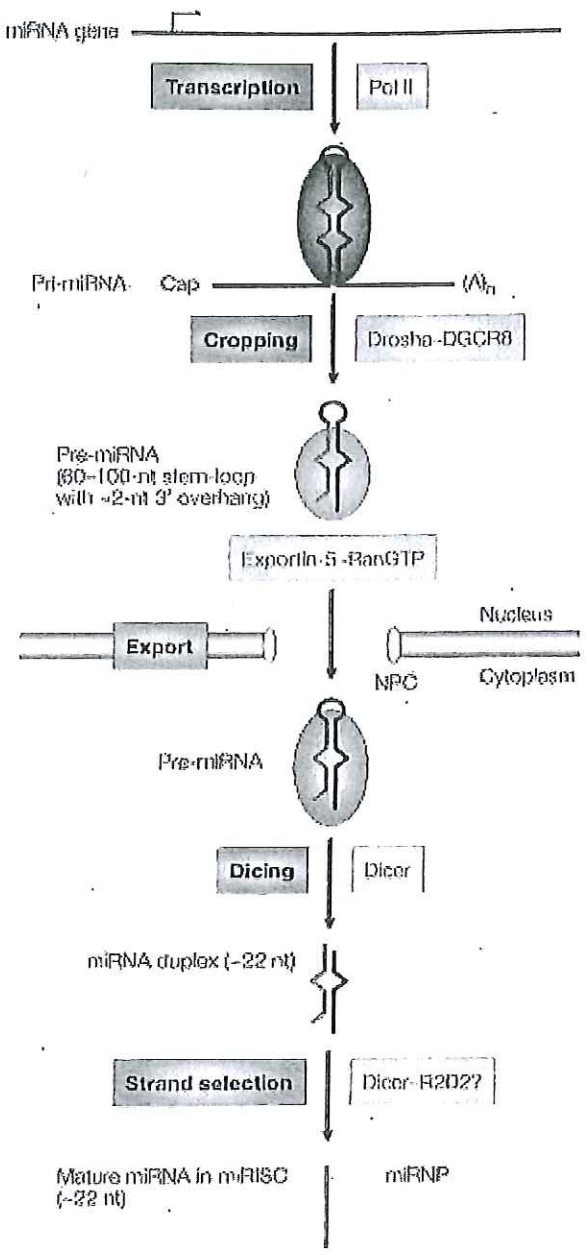

Fig 2. miRNAs are transcribed as long primary transcipts that contain a local hairpin structure. The stem-loop is cleaved in the nucleus by Rnase-III Drosha to create a precursor of miRNA (pre-miRNA). Pre-miRNA is then exported into the cytoplasm where it is processed into a mature miRNA duplex by cytoplasmic Rnase-III enzyme Dicer. Mature miRNAs become incorportaed into effector complexes called miRNA-containing RNA-induced silencing complex (miRISC).

Figure taken from: http://www.nature.com/nrm/journal/v6/n5/fig_tab/nrm1644_F2.html

1.6 miRNAs in cancer

The miRNA-mediated method of gene regulation has crucial roles in a variety of biological processes, such as apoptosis, cell growth and metabolism and organ development [47-49]. Deregulation of miRNAs is therefore likely to contribute to the up or down regulation of proto-oncogenes and tumour suppressor genes involved in cancer carcinogenesis and progression [50]. Indeed, miR-365a-3p which targets Cyclin D1 and Bcl-2 to inhibit cell cycle progression and promote apoptosis, has been shown to be downregulated in colon cancer [51]. Furthermore, miR-124-3p targets SLUG to regulate epithelial-mesenchymal transition in the metastasis of breast cancer, and its expression is significantly repressed in breast cancer cells [52]. miRNAs therefore are a potential therapeutic target in cancer treatment.

A series of microarrays and gene expression analysis studies also reveal that many miRNAs are deregulated in thyroid cancer [35, 53-56]. Analysis of human thyroid tumour tissue revealed subsets of miRNAs that were either up or down regulated in PTC compared to normal thyroid tissue, and that the extent of this up or down regulation correlated with the degree of aggressiveness of the PTC [57]. Certain miRNAs have also been shown to be upregulated in PTC tumours that directly inhibit the thyroid hormone receptor β (THRβ), an important tumour suppressor gene, contributing to the pathogenesis of PTC [58]. Thus, miRNAs are likely to play a role in the pathogenesis of PTCs by altering gene expression.

In 2012, Li et al provided the first evidence that miRNAs regulate PBF expression [59]. miR-122-5p inhibition was found to up-regulate PBF, which promotes hepatocellular carcinoma (HCC) tumour growth and cell invasion. It may therefore be the case that misregulation of miRNAs that target PBF contributes to the increased PBF expression and subsequent tumourigenic activity observed in thyroid carcinomas.

1.7 Aims and hypothesis

The aim of this study was therefore to determine whether miRNAs play a role in the pathological activity of thyroid cancer cells by upregulating proto-oncogene PBF. I hypothesised that PBF expression is partially mediated by miRNAs, and that miRNA disregulation drives PBF overexpression in thyroid carcinoma. To investigate this, I identified five miRNAs that were likely to target PBF based on sequence similarity to the target gene (PBF) and previous studies that have provided evidence of a miRNA that is misregulated in thyroid cancer or another type of cancer. I measured the expression of these miRNAs in thyroid, breast and cervical cancer cell lines by Taqman PCR to gain a broad understanding of the expression of the selected miRNAs in cancer. I then measured PBF expression at the mRNA and protein level following manipulation of selected miRNA levels. This provided insight as to whether each miRNA targeted PBF and may therefore contribute to the oncogenic activity of the cells.

2. MATERIALS AND METHODS

2.1 Materials

2.1.1 Cell Lines and cell culture

HeLa human cervical cancer cell line was obtained from the Health Protection Agency Culture Collections (HPACC)

TPC-1 human papillary thyroid carcinoma cell line was obtained from Dr Rebecca Schweppe, University of Colorado, US

HCT-116 human colon colorectal carcinoma cell line was obtained from Dr Paul Foster, University of Birmingham, UK.

RPMI 1640(-L-Glutamine) – Sigma-Aldrich, UK

Opti-MEM reduced serum media – Gibco, UK

McCoys – Gibco, UK

2.1.2 Buffers and solutions

RIPA lysis buffer – 1 M tris-HIL pH 7.4, sodium chloride, igepal, 1% sodium deoxycholate, 100 mM EDTA and dH_2O

TBST – 1 M tris-HCl pH 7.6, 5 mM sodium chloride, tween-80 and dH_2O

12% Resolving gel – 1.5 M tris-HCl pH 8.8, 40% polyacrylamide, 10% SDS, 10% APS, TEMED and dH_2O

5% Stacking gel – 0.8 M tris-HCl pH 6.8, 40% polyacrylamide, 10% SDS, 10% APS, TEMED and dH_2O

Gel sample buffer – 10% w/v DTT in laemlli buffer

10x Running buffer – tris base, glycine, SDS and dH_2O. Dilute to 1x in dH_2O

Transfer buffer – tris base, glycine, methanol, SDS and dH_2O

2.1.3 Additional materials

Penecillin-streptomycin – GIBCO, UK #1507-063

DL-Dithiothreitol (DTT) – Sigma, UK #D9779-10G

Phophate buffered saline (PBS) tablets – Sigma, UK #P4417-100TAB

Tween-80 – Sigma, UK #P4780

Protogel – National diagnositics, US - #EC-891

Methanol – VWR, UK #20847.307

Trypsin/EDTA – Invitrogen, UK #15400-054

HiPerFect transfection reagent – Qiagen, UK #301702

Precision plus protein dual colour standards – Biorad, US #161-0374

Laemlli sample buffer – Biorad, US #161-0737

Amersham ECL plus western blotting detection system – GE life sciences, UK #RPN2132

TEMED – Sigma, UK #T9281

Sodium chloride – Fischer scientific, UK #S/3160/65

Medical X-ray film – Kodak, US #8143059

Sodium dodecyl sulphate (SDS) - Sigma, UK #L4390

Ammonium persulphate (APS) – Sigma, UK #A3678

2x GoldStar TaqMan PCR mastermix – Eurogenetec, US, #RT-QP2X-03+GQS

Reverse transcription system – Promega, US #A3500

AMV reverse transcriptase – IBR strores, UK #C1181

Random primers – IBR stores, UK #M9004

Protease inhibitor cocktail – Sigma, UK #P8340

Foetal calf serum – Sigma, UK #10437-028

Amersham Hybond P PVDF membrane – GE life sciences, UK #RPN303F

AllStars negative control siRNA – Qiagen, UK

Anti-PBF siRNA – Life technologies #0004602979 Mature sequence: 5'-CAGAAAACCUUCAUAUAATT-3'

miR-122-5p mimic – Qiagen, UK #MSY0000421 Mature sequence: 5'-UGGAGUGUGACAAUGGUGUUUG-3'

miR-124-3p mimic – Qiagen, UK #MSY0000422 Mature sequence: 5'-UAAGGCACGCGGUGAAUGCC-3'

miR-365a-3p mimic – Qiagen, UK #MSY0000710 Mature sequence: 5'UAAUGCCCCUAAAAAUCCUUAU-3'

miR-506-3p mimic – Qiagen, UK #MSY0002878 Mature sequence: 5'UAAGGCACCCUUCUGAGUAGA-3'

miR-647 mimic – Qiagen, UK #MSY0003317 Mature sequence:

5'GUGGCUGCACUCUCACUUCCUUC-3'

2.2 Methods

2.2.1 Cell culture

TPC-1 cells were cultured in RPMI medium (Gibco) with 10% foetal bovine serum (FBS) (Gibco). HCT-116 cells were cultured in McCoy's medium 10% FBS (GIBCO). HeLa cells were cultured in Dulbecco's medium 10% FBS. All cell lines were incubated in a humidified atmosphere with 5% CO_2 at 37 ^{o}C. For routine cell culture, 1:10 (HeLa) and 1:20 (HCT-116, TPC-1) dilutions were carried out. The appropriate volume of cell suspension was transferred to fresh, pre-warmed media in a 75 cm^3 tissue culture flask.

For transfection experiments, Hela cells were plated at 150,000 cells/well for a 6 well plate and 75,000 cells/well for a 12 well plate, and HCT-116 and TPC-1 cells were plated at 200,000 cells/well for a 6 well plate, 100,000 cells/well for a 12 well plate and 50,000 cells/well for a 24 well plate. Cells were always plated 24 hours prior to transfection to adhere at 37 ^{0}C with 5% CO_2.

2.2.2 Transient transfection of TPC-1 cells

24 hours after plating, cells were transfected with either one of five miRNA mimics, AllStars negative control siRNA (Allstars) or anti-PBF siRNA all at 50 nM. Manufacturer's recommended optimal transfection conditions were used. This was HiPerFect transfection reagent at a ratio of 6 µl HiPerFect to 1.5 µl or the appropriate treatment (miRNA mimic, negative control siRNA or anti-PBF siRNA). Prior to transfection, HiPerFect and the appropriate treatment were diluted in opti-MEM, vortexed and incubated at room temperature for 10 minutes to enable complex formation.

100 µl of this transfection mix was then added in a drop-wise manner to each well. Cells were then incubated for a further 48 hours at 37 ^{0}C with 5% CO_2. When downstream analysis was by PCR, cells were plated in 24 well plates in 0.5 ml of media. When downstream analysis was by western blotting, cells were plated in 6 well plated in 2 ml of media.

Cells were transfected with 50 nM miRNA mimic (Qiagen), AllStars negative control (Qiagen) or anti-PBF siRNA (Life technologies). HiPerFect transfection reagent was added at 12 µl for a 6 well plate, 6 µl for a 12 well plate and 3 µl for a 24 well plate.

2.2.3 RNA extraction

Total RNA, including miRNA, was isolated using TRIzol reagent (Ambicon) according to the manufacturer's instruction. The RNA was reverse transcribed using the avian myeloblastosis virus (AMV) Reverse Transcription System (Promega). 0.5 µg of total RNA was diluted in RNase-free water to give a total volume of 5 µl. Samples were then incubated at 70 ^{0}C for 10 minutes. A reverse transcription mastermix was prepared, of which 5 µl was added to each RNA sample. Samples were then incubated at room temperature for a further 15 minutes before they were PCR amplified (42 ^{0}C for 1 hour, 95 ^{0}C for 5 minutes, 4 ^{0}C for 5 minutes). 40 µl of RNase-free water was added to each sample. Samples were pulse spun and stored at -20 ^{0}C.

2.2.4 Quantitative PCR

PBF expression following transfection was determined by quantitative PCR using a 7500 ABI qPCR machine. The PCR reaction was conducted in 96 well PCR plates. 2 µl of cDNA was added to each well. A mastermix was then prepared containing 2x TaqMan universal PCR master mix, a TaqMan gene expression array (PBF or internal control) and RNase-free water. 18 µl of mastermix was then added to each well to give a total reaction volume of 20 µl. Each sample was run in duplicate and expression data were normalised to the internal control 18s. The target gene (PBF) probes were labelled with FAM and the 18s RNA probe with VIC. The PCR reaction was then run

(50 ^{0}C for 2 minutes, 95 ^{0}C for 10 minutes, 40 cycles of 95 ^{0}C for 15 seconds each, 60 ^{0}C for 1 minute). Relative expression levels were calculated using the ΔΔCt method.

2.2.5 Protein extraction

250 µl/well of RIPA lysis buffer containing protease inhibitor cocktail was added to the cells and incubated at -20 ^{0}C for a minimum of 20 minutes. Whole cell lysates were then harvested and protein concentration was determined using Bicichoninic acid (BCA) assay using bovine serum albumin (BSA) as a standard. Lysates were diluted to the appropriate concentration to give a constant protein concentration across samples. Samples were solubilised by laemlli buffer containing 10% DTT at 95 ^{0}C for 10 minutes and stored at -20 ^{0}C.

2.2.6 Western blotting

SDS-PAGE was used for Western blot analysis. Soluble protein samples were placed onto a 12% SDS-polyacrylamide gel alongside a molecular weight marker and electrophoresed at 140 V until the proteins were fully separated. Gels were then placed with a PVDF membrane in a blot cassette which was run for approximately 75 minutes at 360 mA to transfer proteins from the gel to the PVDF membrane. Membranes containing protein were then incubated at room temperature in 5% milk in TBST for 1 hour on an orbital rocker. Membranes were then incubated overnight with the primary antibody diluted in 5% milk in TBST at 4 ^{0}C. The following primary antibodies were used: Rabbit anti-PBF (made in-house) at 1:500, murine monoclonal anti-β-actin AC-15 (Sigma) at 1:10,000. After washing 3 times with TBST for 10 minutes, the membranes were incubated with the appropriate horseradish peroxidase-conjugated secondary antibody diluted in 5% milk in TBST at room temperature for 1 hour. The following secondary antibodies were used: goat anti-rabbit secondary antibody (Dako) at 1:2000, rabbit anti-murine secondary antibody (Dako) at 1:2000. Membranes were then washed again 3 times in TBST for 10 minutes and developed using ECL treatment and subsequent exposure on X-ray film, which was developed by the Xograph Compact X4 X-ray film processor.

2.2.7 Statistical analysis

Data are all displayed as mean $\pm$ sem. Normally distributed data were statistically analysed using a two-tailed Student's *t*-test. A p value of <0.05 was considered to be statistically significant. All data analysis was carried out in Microsoft Excel 2010.

3. RESULTS

3.1 Selection of miRNAs likely to target PBF

Before beginning any functional investigation, I first needed to determine a set of miRNAs that were likely to target the PBF gene. I identified potential target miRNAs based on 3 criteria:

1. Previous experimental validation of targeting PBF
2. Sequence similarity between the miRNA and a site on the 3'UTR of PBF giving rise to complementary base pairing
3. Highly conserved sequence suggesting important evolutionary function

To determine the likelihood of a PBF binding site by sequence similarity and sequence conservation, I employed a computational miRNA target prediction method. This involved searching online databases DIANA-microT, TargetScan, miRanda and MirTarget2 (Table 1) in which computational algorithms have been developed to predict pre-miRNAs [60] and to search for homologous conserved miRNA genes across several animal species. These target prediction programs typically use complementary base pairing pattern, evolutionary conservation and nucleotide composition of the target sequences to identify likely potential targets [61, 62].

miR-122-5p

miR-122-5p is an abundant, liver specific miRNA involved in a variety of hepatic functions and neoplastic transformation [59]. In 2012, Li et al provided the first evidence that PBF is regulated by miRNAs and identified PBF as a target of miR-122-5p [59]. It was also found that miR-122-5p levels were decreased and PBF expression was subsequently increased in chronic hepatitis B (CHB) and hepatocellular carcinoma (HCC) [59]. miR-122-5p was not identified as a potential binding partner of PBF on various prediction websites used (Fig 3). However, miR-122-5p may be a false negative in a database search due to the limited accuracy of computational target prediction

a) **Gene 754 is predicted to be targeted by 36 miRNAs in miRDB**

Target Detail	Target Rank	Target Score	miRNA Name	Gene Symbol	Gene Description
Details	1	88	hsa-miR-186-3p	PTTG1IP	pituitary tumor-transforming 1 interacting protein
Details	2	84	hsa-miR-647	PTTG1IP	pituitary tumor-transforming 1 interacting protein
Details	3	78	hsa-miR-4299	PTTG1IP	pituitary tumor-transforming 1 interacting protein
Details	4	78	hsa-miR-374c-5p	PTTG1IP	pituitary tumor-transforming 1 interacting protein
Details	5	78	hsa-miR-4474-3p	PTTG1IP	pituitary tumor-transforming 1 interacting protein
Details	6	75	hsa-miR-2861	PTTG1IP	pituitary tumor-transforming 1 interacting protein
Details	7	75	hsa-miR-655	PTTG1IP	pituitary tumor-transforming 1 interacting protein
Details	8	72	hsa-miR-5001-5p	PTTG1IP	pituitary tumor-transforming 1 interacting protein
Details	9	71	hsa-miR-4494	PTTG1IP	pituitary tumor-transforming 1 interacting protein
Details	10	68	hsa-miR-3163	PTTG1IP	pituitary tumor-transforming 1 interacting protein
Details	11	67	hsa-miR-506-3p	PTTG1IP	pituitary tumor-transforming 1 interacting protein
Details	12	65	hsa-miR-4797-5p	PTTG1IP	pituitary tumor-transforming 1 interacting protein
Details	13	62	hsa-miR-511	PTTG1IP	pituitary tumor-transforming 1 interacting protein
Details	14	62	hsa-miR-124-3p	PTTG1IP	pituitary tumor-transforming 1 interacting protein
Details	15	61	hsa-miR-100-3p	PTTG1IP	pituitary tumor-transforming 1 interacting protein
Details	16	61	hsa-miR-26a-2-3p	PTTG1IP	pituitary tumor-transforming 1 interacting protein
Details	17	59	hsa-miR-1253	PTTG1IP	pituitary tumor-transforming 1 interacting protein

b) **Human PTTG1IP (NM_004339) 3' UTR miRNA Table**

Table sorted by total context score (Sort table by aggregate P_{CT})

miRNA families broadly conserved among vertebrates

miRNA	conserved sites				poorly conserved sites				Total Context score	Aggregate P_{CT}
	Total	8mer	7mer-m8	7mer-1A	Total	8mer	7mer-m8	7mer-1A		
miR-124/124ab/506	1	1	0	0	0	0	0	0	-0.43	0.92
miR-451	0	0	0	0	1	0	1	0	-0.34	< 0.1
miR-217	0	0	0	0	1	1	0	0	-0.29	< 0.1
miR-196abc	0	0	0	0	1	0	1	0	-0.25	< 0.1
miR-193/193b/193a-3p	0	0	0	0	1	0	1	0	-0.24	< 0.1
miR-33a-3p/365/365-3p	1	0	1	0	0	0	0	0	-0.21	0.24
miR-143/1721/4779	0	0	0	0	1	0	1	0	-0.18	0.11
miR-1ab/206/613	0	0	0	0	1	0	1	0	-0.16	< 0.1
miR-184	0	0	0	0	1	0	0	1	-0.11	< 0.1
miR-216b/216a-5p	0	0	0	0	1	0	1	0	-0.10	< 0.1
miR-26ab/1297/4465	0	0	0	0	1	0	0	1	-0.09	< 0.1
miR-192/215	0	0	0	0	1	0	1	0	0.09	< 0.1
miR-223	0	0	0	0	1	0	1	0	-0.06	< 0.1
miR-205/205ab	0	0	0	0	1	0	0	1	-0.04	< 0.1
miR-338/338-3p	0	0	0	0	1	0	0	1	-0.03	< 0.1
miR-29abcd	0	0	0	0	1	0	1	0	-0.02	< 0.1

c)

Conserved

		predicted consequential pairing of target region (top) and miRNA (bottom)	seed match	site type contribution	3' pairing contribution	local AU contribution	position contribution	TA contribution	SPS contribution	context+ score	context+ score percentile	conserved branch length
Position 1938-1945 of PTTG1IP 3' UTR	5'	...ACCAUAAAGCUUGGAGUGCCUUA...	8mer	-0.247	0.003	-0.046	-0.101	0.021	-0.059	-0.43	99	2.112
hsa-miR-506	3'	AGAUGAGUCUUCCCACGGAAU										
Position 1938-1945 of PTTG1IP 3' UTR	5'	...ACCAUAAAGCUUGGAGUGCCUUA...	8mer	-0.247	0.013	-0.046	-0.101	0.021	-0.059	-0.42	98	2.112
hsa-miR-124	3'	CCGUAAGUGGCGCACGGAAU										

Context+ score and features that contribute to the context+ score are evaluated as in Garcia et al. 2011.

Conserved branch length and P_{CT} are evaluated as in Friedman et al. 2009.

d)

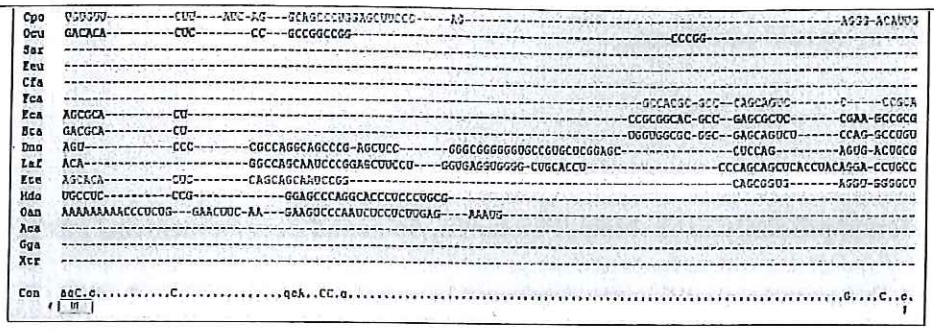

Conserved

	predicted consequential pairing of target region (top) and miRNA (bottom)		seed match	site-type contribution	3' pairing contribution	local AU contribution	position contribution	TA contribution	SPS contribution	context+ score	context+ score percentile	conserved branch length
Position 1895-1901 of PTTG1IP 3' UTR	5'	...UGAAAUACACUAAGAGCAGCCAC...	7mer-m8	-0.120	0.003	-0.055	-0.048	0.010	-0.084	-0.29	91	1.515
hsa-miR-647	3'	CUUCCUUCACUCACGUCGGUG										

Context+ score and features that contribute to the context+ score are evaluated as in Garcia et al, 2011.

Conserved branch lengths and P_{CT} are evaluated as in Friedman et al, 2009.

e)

Conserved

	predicted consequential pairing of target region (top) and miRNA (bottom)		seed match	site-type contribution	3' pairing contribution	local AU contribution	position contribution	TA contribution	SPS contribution	context+ score	context+ score percentile	conserved branch length
Position 1602-1609 of PTTG1IP 3' UTR	5'	...UUUCCCUGACCUCUUGGGCAUUU...	7mer-m8	-0.120	0.012	-0.052	-0.007	-0.015	-0.032	-0.21	80	1.912
hsa-miR-365	3'	UAUUCCUAAAAAUCCCCGUAAU										

Context+ score and features that contribute to the context+ score are evaluated as in Garcia et al, 2011.

Conserved branch lengths and P_{CT} are evaluated as in Friedman et al, 2009.

Fig 3. Computational method of miRNA target prediction. Justification of selection of miR-124-3p, miR-365a-3p, miR-506-3p and miR-647 as potential PBF regulators. a) Table of miRNAs predicted to have binding sites with PBF in order of probability from miRTarget2 website. miR-647, miR-506-3p-3p and miR-124-3p-3p are highlighted by red boxes. b, c) miR-124-3p and miR-506-3p are identified by TargetScan as being broadly conserved amongst vertebrates and the most likely targets of PBF based on nucleotide sequence. d, e) miR-647 and miR-365a-3pa-3p are identified by TargetScan as being conserved amongst vertebrates and likely targets of PBF based on nucleotide sequence.

methods. However, since it is a validated PBF regulator, I selected miR-122-5p as a potential regulator of PBF in thyroid carcinoma.

miR-124-3p

miR-124-3p is found primarily in the brain, functioning in neural development and gastrulation [63]. It has been shown to be significantly decreased in a variety of tumours including medulloblastoma, oral squamous cell carcinomas and HCC, suggesting a possible tumour suppressive role for miR-124-3p in carcinogenesis [64-66]. It was also recently found to be pathologically downregulated in breast cancer specimens and cell lines, resulting in increased cell motility and invasion capability via subsequent upregulation of it's target SLUG, an epithelial-mesenchymal transition (EMT) regulator [52]. miR-124-3p was also regularly identified as potential targeting PBF by the prediction websites (Fig 3). Microarray analysis also validated miR-124-3p as targeting PBF [67].

miR-365a-3p

miR-365a-3p is a relatively poorly characterised miRNA. However, there is evidence that it exhibits a tumour suppressive role in oncogenesis, and is downregulated in a number of cancers. For example, miR-365a-3p was reported to be downregulated in the growth arrest phase of quiescence and senescence in lung fibroblasts [68]. It has also been found to be downregulaed in colon cancer, where it targets Cyclin D1 and Bcl-2 to inhibit cell cycle progression and apoptosis [51]. It was also found to be highly conserved amongst vertebrates (Fig 3e).

miR-506-3p

miR-506-3p function is also largely elusive. It has, like miR-124-3p, been shown to target SLUG to increase cell motility and invasion in breast cancer [52]. This is logical, since miR-124-3p and miR-506-3p have a similar nucleotide sequence and share a binding site on the PBF 3' UTR (Fig 3). It

has also been shown to play an oncogenic role in melanocyte transformation and promoting melanoma growth [69]. It was also identified as a broadly conserved miRNA amongst vertebrates (Fig 3b-c).

miR-647

miR-647 has been identified as a potential biomarker for several different tumours including prostate and ovarian cancers [70, 71]. It was also picked up as a potential regulator of PBF by numerous databases (fig 3a).

Table 1. Computational methods for miRNA target prediction

Name	URL
DIANA-microT	http://diana.pcbi.upenn.edu/cgi-bin/micro_t.cgi
TargetScan	http://www.targetscan.org/
miRanda	http://www.microrna.org/microrna/home.do
MirTarget2	http://mirdb.org/miRDB/

3.2 miR-122-5p AND miR-124-3p are endogenously expressed in HeLa, HCT-116 and TPC-1 cell lines

Prior to investigating the effect of manipulating the levels of the selected miRNAs in cell lines, I first needed to determine the endogenous expression of the miRNAs in the cell lines. I used a TaqMan PCR to measure the endogenous expression of the miRNAs compared to RNU endogenous control. This was to gain a broad understanding of miRNA expression in cancer cell lines before

focusing specifically on thyroid cell lines. miR-122-5p and miR-124-3p were found to be endogenously expressed in Hela, HCT-116 and TPC-1 cells (Fig 4).

3.3 PBF knock down in HeLa cells occurs with 50nM anti-PBF siRNA

Before transfecting cell lines with miRNA mimics, I first needed to determine the optimal concentration of miRNA mimic to introduce into the cell. Anti-PBF siRNA2233 targets the 3' UTR of PBF, as do miRNAs. Since miRNA mimics are replicas of endogenous miRNAs, which essentially act in a similar manner as siRNA, it seemed logical that the optimal concentration of anti-PBF siRNA for transfection into cell lines would be useful in determining the optimal concentration for transfection with miRNA mimics. I therefore transfected HeLa cells with 100nM anti-PBF siRNA, which has been validated as the optimal concentration with Lipofectamine transfection reagent [15, 17, 72], or 50 nM anti-PBF siRNA, along with HiPerFect transfection reagent. When anti-PBF siRNA was transfected at 100nM, there was an $87.94 \pm 5.30\%$ knockdown of PBF expression compared to the negative control (Fig 5, $p<0.05$). Anti-PBF at 50 nM resulted in an $85.96 \pm 4.51\%$ knockdown of PBF expression compared to the negative control ($p<0.01$). There was therefore only a 1.97% greater PBF knockdown when anti-PBF siRNA was used at 100 nM than at 50 nM. This difference was insignificant ($p>0.05$). I therefore determined 50 nM as the optimal concentration of anti-PBF siRNA to transfect into HeLa cells, and the most likely optimal concentration of miRNA mimics to transfect as well.

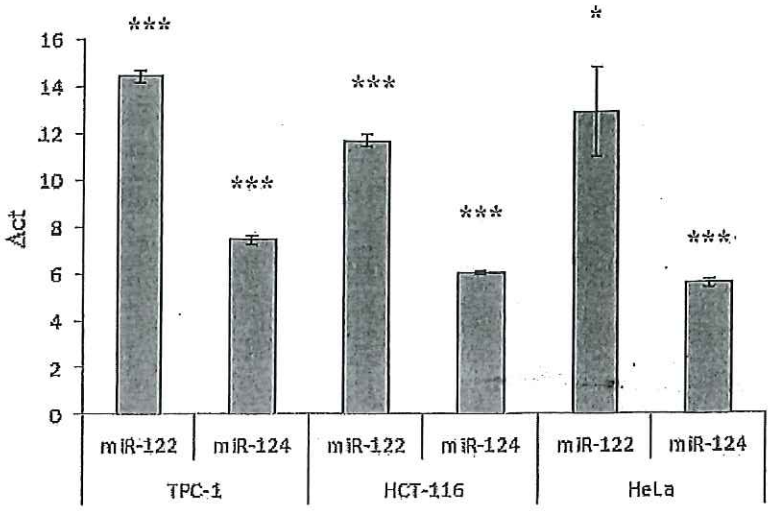

Fig 4. Expression of miR-122-5p and miR-124-3p in HeLa, HCT-116 and TPC-1 cells. For all cell lines, Δct values of relative expression of miR-122-5p and miR-124-3p versus that of endogenous control RNU are represented in the vertical axis. Experiments were performed three times. Data are presented as means ± sem. $P<0.05$ for miR-122-5p and miR124 in all three cell lines by a two-tailed Student's *t*-test.

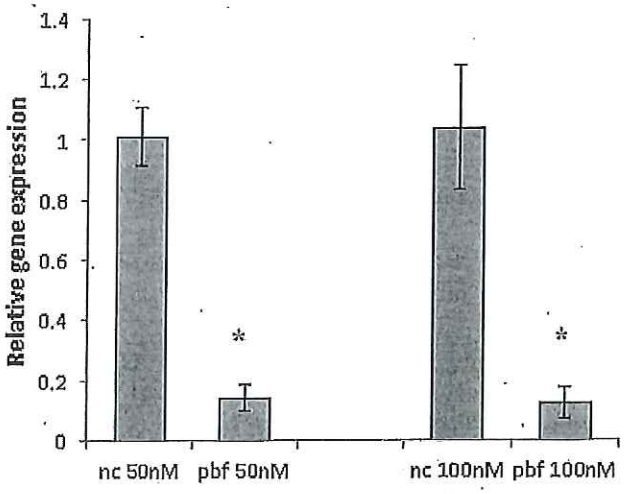

Fig 5. Expression of PBF in HeLa cells transfected 50nM or 100nM anti-PBF siRNA. Fold changes of relative expression of PBF following transfection of either 50nM anti-PBF siRNA or 100nM anti-PBF siRNA with HiPerFect transfection reagent versus cells transfected with 50nM or 100nM of AllStars negative control siRNA respectively are represented in the vertical axis. Experiments were performed three times. Data are presented at means ± sem. $P<0.05$ in both cases by student's *t*-test.

3.4 PBF expression is decreased in TPC cells transfected with mimics of miR-122-5p, miR-124-3p, miR-506-3p and miR-647

After determining the endogenous expression of the miRNAs in Hela, HCT-116 and TPC-1 cells and identifying 50nM as the optimal transfection concentration to use for miRNA mimic transfection in HeLa cells, I then intended to transfect miRNA mimics of miR-122-5p, miR-124-3p, miR-365a-3p, miR-506-3p and miR-647 into HeLa cells at 50nM. I then determined PBF expression at the mRNA level by TaqMan PCR analysis and at the protein level by western blot analysis. This enabled me to speculate as to whether the miRNAs chosen target PBF and regulate PBF expression in these cell lines. miRNAs are thought to downregulate their target gene's expression. Therefore, if the chosen 5 miRNAs do indeed target and regulate PBF expression, I would expect to see a decrease in PBF expression at the mRNA and protein level. However, due to a technical failure with the HeLa cell incubator, HeLa cells were no longer viable for this experiment. I therefore used TPC-1 cells as host cells for transfection with miRNA mimics.

Figure 6 shows PBF expression following transfection with one of seven conditions; AllStars negative control siRNA, anti-PBF siRNA or a mimic of miR-122-5p, miR-124-3p, miR-365a-3p, miR-506-3p or miR-647. Fig 6 a-c (#1, #2 and #3) represents 3 individual repeats of this transfection experiment.

PBF expression was significantly decreased when cells were transfected with anti-PBF siRNA and miR-506-3p mimic (Fig 6b, $p<0.01$, $p<0.05$ respectively). Anti-PBF siRNA tramsfection resulted in a $56.22 \pm 5.46\%$ knockdown of PBF expression, and miR-506-3p mimic transfection resulted in a $49.54 \pm 7.95\%$ PBF knockdown (Fig 6b). A decrease in PBF expression was also observed when cells were transfected with mimics of miR-122-5p ($42.99 \pm 27.25\%$), miR-124-3p ($26.38 \pm 5.20\%$), miR-365a-3p ($28.89 \pm 9.84\%$), or miR-647 ($43.81 \pm 20.66\%$) (Fig 6b). However, none of these decreases were statistically significant ($p>0.05$ in all cases).

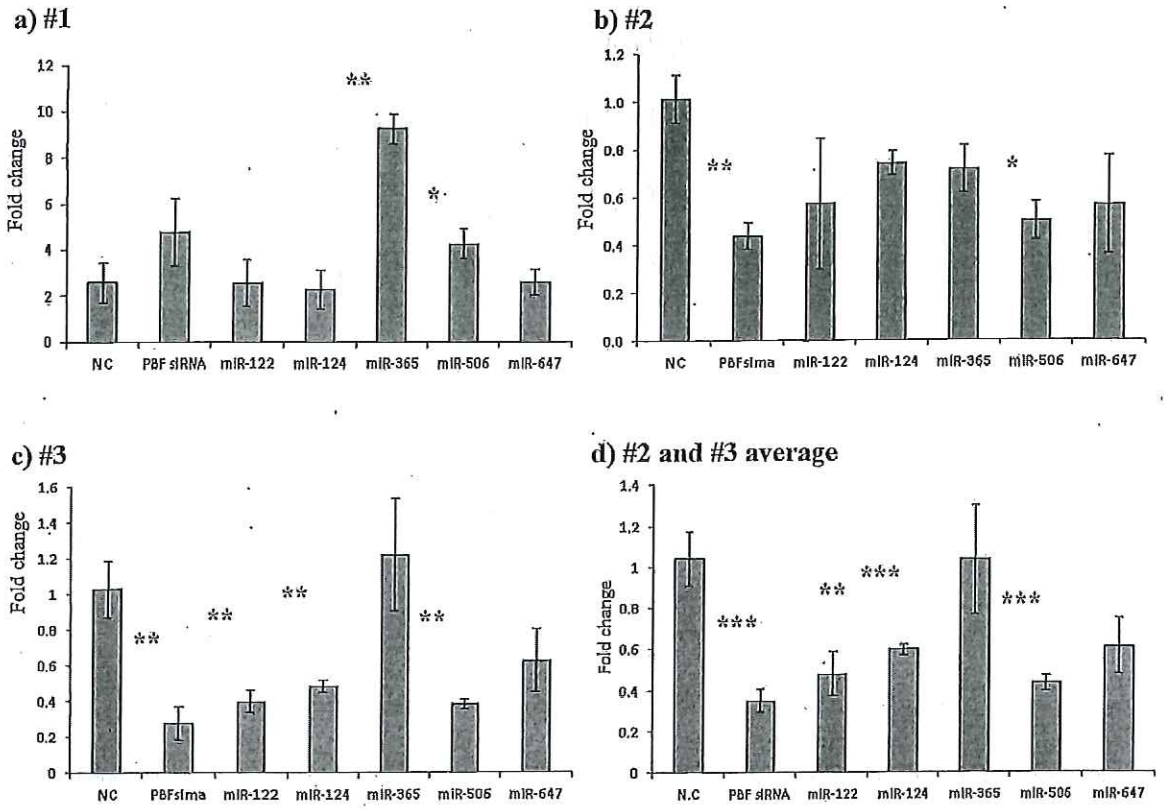

Fig 6. (a-d) Expression of PBF in TPC-1 cells transfected with one of seven treatments: AllStars negative control siRNA, anti-PBF siRNA or miRNA mimics of miR-122-5p, miR-124-3p, miR-365a-3p, miR-506-3p or miR-647. Fold change of relative PBF expression following transfection versus PBF expression versus transfection with negative control siRNA are represented in the vertical axis. a) Repeat one of transfection experiment. PBF expression is significantly different to cells transfected with negative control siRNA in cells transfected with mimics of miR-365a-3p and miR-506-3p ($p<0.05$ in both cases) by a two tailed students *t*-test. b) Repeat two of the transfection experiment. PBF expression is significantly different to cells transfected with negative control siRNA in cells transfected with anti-PBF siRNA and miR-506-3p mimic ($p<0.05$ in both cases) by a two tailed students *t*-test. c) Repeat three of transfection experiment. PBF expression is significantly different to cells transfected with negative control siRNA in cells transfected with anti-PBF siRNA and mimics of miR-122-5p, miR-124-3p and miR-506-3p ($p<0.05$ in all cases) by a two tailed students *t*-test. d) Average of repeats two and three of the transfection experiment. PBF expression is significantly different to cells transfected with negative control siRNA in cells transfected with anti-PBF siRNA and mimics of miR-122-5p, miR-124-3p and miR-506-3p ($p<0.05$ in all cases) by a two tailed students *t*-test.

PBF expression was significantly decreased compared to the negative control when cells were transfected with anti-PBF siRNA (72.50 ± 1.45% PBF knockdown) and mimics of miR-122-5p (60.36 ± 6.43% PBF knockdown), miR-124-3p (52.10 ± 3.27% PBF knockdown) and miR-506-3p (61.76 ± 2.59% PBF knockdown) (Fig 6c, $p<0.05$ in all cases). A decrease in PBF expression was detected when cells were transfected with miR-647 mimic (37.60 ± 17.75%), but this decrease was not significant ($p>0.05$). There was a slight increase in PBF expression when cells were transfected with miR-365a-3p mimic compared to the negative control (21.73 ± 31.53%). However, the extremely large error bars and lack of statistical significance ($p>0.05$) suggest that this was not a genuine result, and that there was minimal change to PBF expression in TPC-1 cells when transfected with miR-365a-3p mimic.

There was a significant change in PBF expression compared to the negative control when cells were transfected with mimics of miR-365a-3p (667.82 ± 66.71% increase in PBF expression) and miR-506-3p (168.05 ± 66.08% increase in PBF expression) ($p<0.05$ in both cases) (Fig 6a). There was no significant decrease when cells were transfected with anti-PBF siRNA or mimics of miR-122-5p, miR-124-3p or miR-647 ($p>0.05$ in all cases). However, this graph does display some abnormalities. miR-365a-3p mimic transfection resulted in a drastic increase in PBF expression (667.82 + 66.71%). Also, transfection with anti-PBF siRNA resulted in a 216 ± 147% increase in PBF expression. However, this anti-PBF siRNA has been previously validated as effectively decreasing PBF expression in TPC cells [17, 73]. Fig 6b and c (#2 and 3) display results that are fairly consistent with each other and are therefore more likely to be accurate, genuine reflections of the molecular events occurring following the transfections than Fig 6a. Fig 6a also represents my first attempt at a miRNA mimic transfection. It was therefore more likely to be less technically accurate and viable than repeats 2 and 3 (Fig 6b-c). I will therefore consider Fig 6a (#1) to be an anomalous result, and the data from this repeat will not be included in the averages of this transfection experiment.

The average PBF expression between repeats 2 and 3 was significantly decreased when cells were transfected with anti-PBF siRNA (65.28 ± 5.56%, $p<0.01$) and mimics of miR-122-5p (52.45 ± 10.6%1, $p<0.05$), miR-124-3p (40.61 ± 2.66%, $p<0.01$) and miR-506-3p (56.96 ± 3.98%, $p<0.01$) (Fig 6d). The greatest statistical significance was seen when cells were transfected with miR-506-3p mimic ($p=0.000493$). A decrease in PBF expression was also observed when cells were transfected with miR-647 mimic (38.94 ± 13.97%), although this decrease was not significant ($p>0.05$). There appeared to be no difference in PBF expression when cells were transfected with miR-365a-3p mimic compared to the negative control (3.29 ± 26.65% increase, $p>0.05$), other than PBF expression became more variable, represented by the relatively large error bars for miR-365a-3p mimic transfection.

Taken together, these data suggest that miR-122-5p, miR-124-3p and miR-506-3p might target and be involved in the regulation of PBF. miR-647 could also target PBF, but miR-365a-3p appears to have no effect on PBF expression and most likely does not target PBF.

3.5 Transfection with miRNA mimics does not affect PBF protein levels

There was no visible difference in PBF protein levels in TPC-1 cells following transfection with miRNA mimics of miR-122-5p, miR-124-3p, miR-365a-3p, miR-506-3p or miR-647, anti-PBF siRNA compared to cells transfected with negative control siRNA (Fig 7a). However, the β-actin loading control showed that unequal amounts of protein were loaded between transfection conditions. Conclusions therefore cannot be readily drawn from Fig 7a. Fig 7b shows the relative density of the blot for each transfection condition compared to the β-actin loading control. The abnormally high value of miR-365a-3p mimic transfection has skewed the axis of fig 7b, making comparisons between relative densities of PBF in other transfection conditions difficult. Fig. 7c shows the same data as fig 7b, but miR-365a-3p mimic transfection results are not plotted.

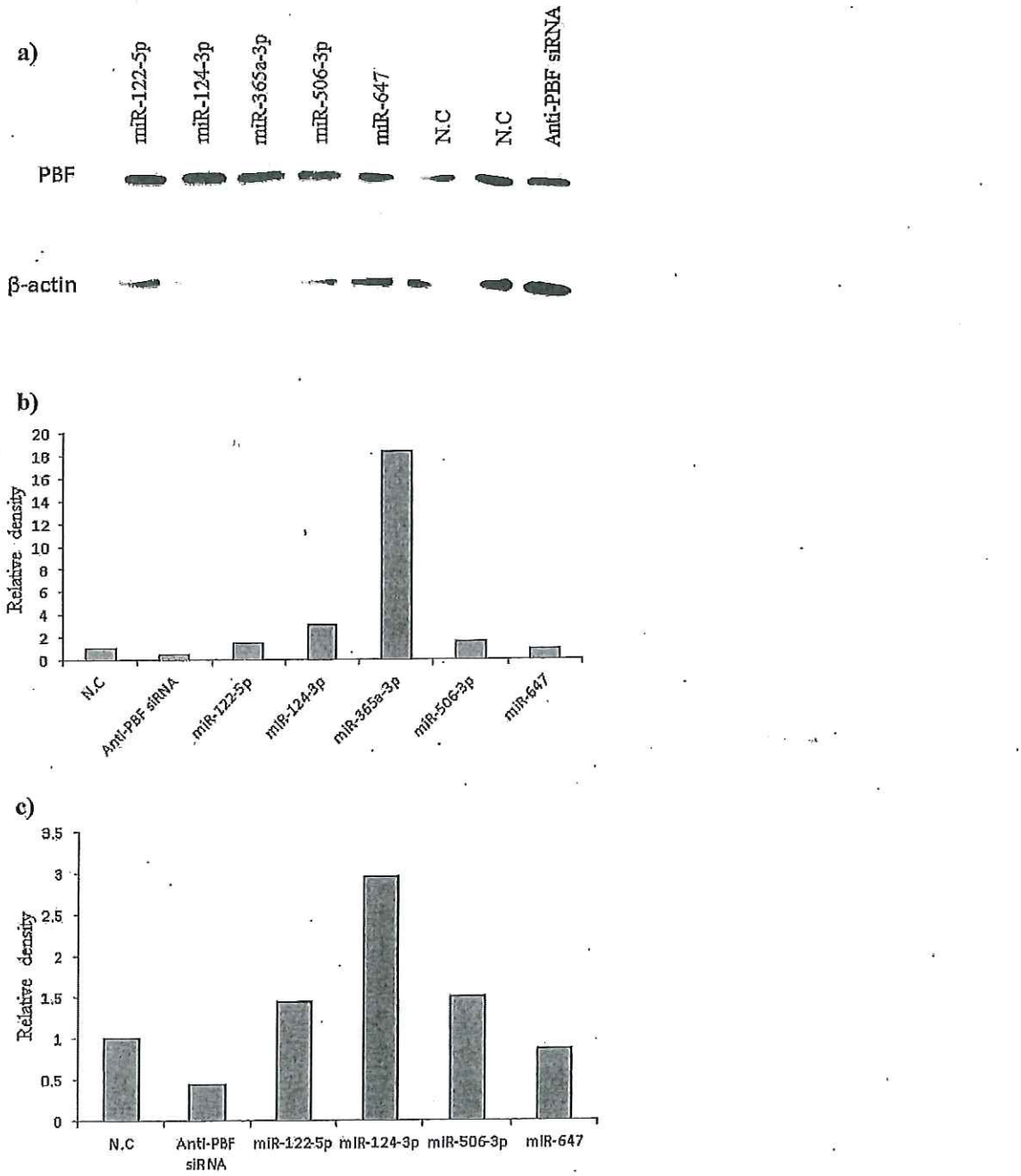

Fig 7. Profiling of PBF protein levels in TPC-1 cells following miRNA mimic transfection. a) TPC-1 cells were harvested 48 hours after transfection with mimics of either miR-122-5p-5p, miR-124-3p-3p, miR-365a-3pa-3p, miR-506-3p-3p or miR-647, anti-PBF siRNA or negative control siRNA. There is no obvious change in PBF protein levels in any condition. B-actin was used as a loading control. However, β-actin protein levels are not similar in all conditions. b) Relative density the blot for each transfection condition compared to the β-actin loading control. Data is presented as fold change in protein levels compared to the average relative density of the two blots for cells transfected with negative control siRNA. c) Relative density the blot for each transfection condition compared to the β-actin loading control. Data is presented as fold change in protein levels compared to the average relative density of the two blots for cells transfected with negative control siRNA. miR-365a-3pa-3p is not plotted as it skews graph 7bb. Error bars are not present since n=1. Statistical analysis was also not possible since n=1.

There is no clear effect on PBF protein levels compared to the negative control when cells were transfected with mimics of miR-122-5p, miR-124-3p, miR-365a-3p or miR-647 (Fig 7c). There was a 56% decrease in PBF expression when cells were transfected with anti-PBF siRNA.

4. DISCUSSION

Deregulation of proto-oncogenes and tumour suppressor genes is a key event underlying the development and pathogenesis of nearly all human carcinomas. PBF is a ubiquitously expressed gene, although its function remains largely unknown. However, previous research has identified PBF as a proto-oncogene involved in transformation and tumourigenesis that is found to be upregulated in many types of cancer, particularly thyroid carcinoma [17, 20]. Regulators of PBF such as miRNAs are therefore also likely to be misregulated in such diseases. miRNAs have now been shown to regulate numerous genes, and in 2012 the first evidence that PBF expression is regulated by miRNAs was published [59]. This provided the rationale for my investigation.

In order to select 5 miRNAs that were likely to target PBF, I employed a computational miRNA target prediction search, which uses complementary base pairing pattern, evolutionary conservation and nucleotide composition of the target sequences to identify likely potential targets [61, 62]. However, in a study into the accuracy of such programs, it was found that precision was ~50% and sensitivity was 6-12% [74]. Using complementary base pairing pattern to detect potential binding sites with target mRNAs has some issues. For example, some miRNAs bind their target mRNA tightly at the 5' and 3' end with a bulge in the middle called a mismatch or wobble where complementary base pairing is not present. These cannot be detected by most target prediction methods, resulting in an increase of false negatives. In terms of conservation analysis, there is also much to consider. For example, with human transcripts it may be more meaningful to search for conserved targets between more distantly related species such as dogs as opposed to closely related ones such as chimpanzees. However, their genomes may not be sequenced along with their evolutionary distance, increasing the likelihood of obtaining false negatives but decreasing false positives. Furthermore, because miRNAs are short and animal miRNAs have limited sequence complementarity to their targets, it is difficult to predict animal miRNA targets with high

specificity. Computational methods of predicting miRNA targets do have some methodological flaws. I therefore looked for several positive factors such as identification as PBF regulators in multiple different databases or high sequence conservation and published evidence to maximise the probability that my selected miRNAs did indeed target PBF. Selecting, for example, 50 miRNAs that appear to be likely to target PBF based on the three search criteria, then performing a TaqMan miRNA assay to identify the five miRNAs that bind most potently with PBF would have been a more accurate selection process and would ensure that all five miRNAs selected did indeed target PBF. However, due to time constraints, this was not feasible.

Fig 4 shows that selected miRNAs miR-122-5p and miR-124 are endogenously expressed in HeLa, HCT-116 and TPC-1 cells. I used a TaqMan PCR to measure mRNA expression of PBF when cells were transfected with various miRNA mimics compared to RNU endogenous control. However, there is currently no established control for miRNA profiling. Let-7a, 18s, RNU and GMN are commonly used as housekeeping genes [75]. I chose to use RNU as my endogenous control for this experiment. RNU is predicted to guide the 2'O-ribose methylation of 28S RNA [75]. However, a more accurate method of selecting an appropriate endogenous control would be to test several candidate control genes and chose one with lowest fluctuation in expression levels. I also employed a singleplex PCR technique to compare the mRNA levels of PBF when cells were transfected with various miRNA mimics. Separate wells containing a 2 µl aliquot of the same sample were measured for PBF expression to RNU expression. Performing a multiplex PCR in which the same aliquot would have been measured for both PBF expression and RNU expression would have minimised pipetting errors between samples and been a more accurate determination of PBF expression. However, given the high level of significance in every case, it can be concluded that miR-122-5p and miR-124-3p are extremely likely to be expressed in Hela, HCT-116 and TPC-1 cells.

Before transfecting cell lines with miRNA mimics, I first needed to determine the optimal concentration of miRNA mimic to transfect. I identified 50 nM as the optimal concentration of anti-

PBF siRNA and miRNA mimic to transfect into HeLa cells (Fig 5). While there was minimal difference between the level of PBF knockdown at 50 nM and 100 nM, using a lower concentration would mean less toxicity to the cells, reduced likelihood of off-target effects and better validation of the efficiency of the miRNA mimics, since administering a large dose such as 100 nM is likely to induce an intracellular response whether that miRNA specifically targets PBF or not. However, this was validated in HeLa cells and the transfection of miRNA mimics was done in TPC-1 cells. This was because, due to a technical failure with the HeLa cell incubator, HeLa cells were no longer viable for transfection. Due to time constraints, I did not determine the optimal transfection concentration in TPC-1 cells. This could have meant that I was not administering the optimal concentration of miRNA mimics for transfection into TPC-1 cells.

Fig 6d shows that PBF expression was significantly reduced in TPC-1 cells when cells were transfected with miRNA mimics of miR-122-5p, miR-124-3p and miR-506-3p. This suggests that in untreated cells, endogenous miR-122-5p, miR-124-3p and miR-506-3p target and are capable of regulating the expression of PBF. PBF is a proto-oncogene that is significantly upregulated in thyroid carcinoma [17, 20]. I hypothesised that this upregulation may be due to deregulation of the miRNAs that regulate PBF. miRNAs generally downregulate the expression of their target gene by translational repression and/or mRNA degradation. It may therefore be the case that, in thyroid carcinoma cells, miRNAs that target PBF, including miR-122-5p, miR-124-3p and miR-505, are downregulated, resulting in a subsequent upregulation of PBF.

These results are in accordance with those of Li et al, who were the first to prove that PBF is regulated by miRNAs, specifically miR-122-5p [59]. It was found that miR-122-5p levels were decreased and PBF was subsequently upregulated in human tissue samples of CHB and HCC. They too found that transfection with miR-122-5p mimic decreased PBF expression, and also that inhibition of endogenous miR-122-5p with a miR-122-5p inhibitor caused increased PBF expression in Huh-7 cells. This combined with my own data lead me to strongly believe that miR-

122-5p does indeed target PBF and regulate its expression. Furthermore, Li et al showed that PBF silencing resulted in a drastic reduction of HCC tumour growth in vivo, highlighting a promising potential for targeted PBF treatment for such diseases [59]. However, in order to conclude that the downregulation of miR-122-5p in human thyroid carcinoma cells causes the increased PBF expression observed, much further work needs to be done.

Transfection with miR-647 mimic did appear to decrease PBF expression, but not significantly ($p>0.05$). The decrease in PBF expression may be due to a random, off-target effect. However, deregulation of genetic factors, epigenetic factors, transcriptional factors and signalling pathways are all likely to contribute to the pathogenesis of thyroid carcinoma. PBF is likely to be one gene amongst many involved in the tumourigenesis process and miR-647 is likely to be one of many miRNAs and other intracellular molecules regulating its expression. Merely increasing the levels of miR-647 in this process may have had less of an effect on PBF expression than other miRNAs that regulate PBF more strongly, hence the lack of statistical significance. There may be other molecules in a possible signalling pathway involving miR-647 and PBF that compensate for the increased miR-647 expression when miR-647 mimics were introduced into the cells. Much deeper understanding of the signalling pathways involving PBF is needed before accurate and validated conclusions can be drawn about the role of miRNAs in regulating PBF expression in thyroid carcinoma.

Fig 7 revealed that levels of PBF protein were not decreased following transfection with miRNA mimics. When cells were transfected with miR-365a-3p mimic, there was an 18 fold increase in PBF expression. This value is likely to be so high because very little β-actin was detected in these cells. However, since PBF protein levels appear to be relatively similar to the other lanes, I suspect that this blot does not reflect β-actin protein levels in the cells. A bubble during transfer could have caused the protein to not adhere to the membrane and therefore not be detected by the anti-β-actin

antibody. The relative density value for PBF following miR-365a-3p mimic transfection may therefore be an anomaly.

The lack of PBF protein level decrease in TPC-1 cells transfected with miR-122-5p, miR-124-3p and miR-506-3p is not in accordance with the results displayed in fig 6, where PBF expression is decreased following mimic transfection. However, PCR analysis of PBF expression at the mRNA level (Fig 6) and western blot analysis of PBF protein levels (Fig 7) were both carried out 48 hours post transfection. If PBF is a relatively stable protein, it may take longer than 48 hours for the downregulation of PBF to be seen at the protein level. I therefore should have analysed PBF protein levels at various time points post transfection. However, due to time restraints this was not possible.

5. FURTHER WORK

In order to conclude that the downregulation of miR-122-5p in human thyroid carcinoma cells causes the increased PBF expression observed, I would first need to repeat the miRNA mimic transfection experiment many more times to increase the n number and therefore validity of results. I would also need to repeat the experiment in a number of different cell lines, since I only performed the transfection in TPC cells and cell lines inevitably differ in terms of transfection efficiency and endogenous gene expression. I would then need to inhibit endogenous miR-122-5p expression in TPC-1 cells and observe the effect that this had on PBF expression. If PBF expression increased then it is likely that endogenous miR-122-5p does regulate PBF expression in thyroid carcinoma, since TPC-1 cells are a thyroid cancer cell line. I would then need to measure miR-122-5p expression in human thyroid carcinoma primary tissue samples compared to non-cancerous tissue. If miR-122-5p was consistently found to be at lower levels in thyroid carcinoma tissue, where PBF is upregulated, this would strongly suggest that downregulation of miR-122-5p contributes to the upregulation of PBF and subsequent pathogenesis of thyroid carcinoma. Targeting the miRNAs that regulate PBF in thyroid carcinoma treatment would then have therapeutic potential. *In vivo* studies have shown that downregulation or silencing altogether of PBF does cause decreased tmourigenesis in various tumours [51, 52, 59]. *In vivo* investigation as to whether restoring the correct regulation of the miRNAs that regulate PBF caused decreased tumourigenesis in thyroid carcinoma would be necessary to prove any clinical relevance of the findings of the present study, since deregulation of genetic factors, epigenetic factors, transcriptional factors and signalling pathways are all likely to contribute to thyroid carcinogenesis.

REFERENCES

1. Hunt, P.J., et al., *Histocompatibility leucocyte antigens and closely linked immunomodulatory genes in autoimmune thyroid disease.* Clinical endocrinology, 2001. **55**(4): p. 491-9.
2. *Thyroid Cancer Statisics-Key Facts*. 2012 01/05/2013]; Available from: http://info.cancerresearchuk.org/cancerstats/types/thyroid/incidence/#trends.
3. Mazzaferri, E.L. and R.T. Kloos, *Clinical review 128: Current approaches to primary therapy for papillary and follicular thyroid cancer.* The Journal of clinical endocrinology and metabolism, 2001. **86**(4): p. 1447-63.
4. Mazzaferri, E.L., *Finding and treating subclinical hypothyroidism.* Hospital practice, 2001. **36**(6): p. 9-10, 16.
5. Grodski, S., et al., *Increasing incidence of thyroid cancer is due to increased pathologic detection.* Surgery, 2008. **144**(6): p. 1038-43; discussion 1043.
6. Mazzaferri, E.L., *Histologic variants of papillary thyroid carcinoma.* Endocrine practice : official journal of the American College of Endocrinology and the American Association of Clinical Endocrinologists, 2001. **7**(2): p. 139-42.
7. Rivera, M., et al., *Molecular genotyping of papillary thyroid carcinoma follicular variant according to its histological subtypes (encapsulated vs infiltrative) reveals distinct BRAF and RAS mutation patterns.* Modern pathology : an official journal of the United States and Canadian Academy of Pathology, Inc, 2010. **23**(9): p. 1191-200.
8. Smallridge, R.C., L.A. Marlow, and J.A. Copland, *Anaplastic thyroid cancer: molecular pathogenesis and emerging therapies.* Endocrine-related cancer, 2009. **16**(1): p. 17-44.
9. Jemal, A., et al., *Cancer statistics, 2008.* CA: a cancer journal for clinicians, 2008. **58**(2): p. 71-96.
10. Barril, N., A.B. Carvalho-Sales, and E.H. Tajara, *Detection of numerical chromosome anomalies in interphase cells of benign and malignant thyroid lesions using fluorescence in situ hybridization.* Cancer genetics and cytogenetics, 2000. **117**(1): p. 50-6.
11. Taruscio, D., et al., *Numerical chromosomal aberrations in thyroid tumors detected by double fluorescence in situ hybridization.* Genes, chromosomes & cancer, 1994. **9**(3): p. 180-5.
12. Kimura, E.T., et al., *High prevalence of BRAF mutations in thyroid cancer: genetic evidence for constitutive activation of the RET/PTC-RAS-BRAF signaling pathway in papillary thyroid carcinoma.* Cancer research, 2003. **63**(7): p. 1454-7.
13. Soares, P., V. Maximo, and M. Sobrinho-Simoes, *Molecular pathology of papillary, follicular and Hurthle cell carcinomas of the thyroid.* Arkhiv patologii, 2003. **65**(2): p. 45-7.
14. Frattini, A., et al., *Chloride channel ClCN7 mutations are responsible for severe recessive, dominant, and intermediate osteopetrosis.* Journal of bone and mineral research : the official journal of the American Society for Bone and Mineral Research, 2003. **18**(10): p. 1740-7.
15. Smith, V.E., et al., *PTTG-binding factor (PBF) is a novel regulator of the thyroid hormone transporter MCT8.* Endocrinology, 2012. **153**(7): p. 3526-36.
16. Smith, V.E., J.A. Franklyn, and C.J. McCabe, *Expression and function of the novel proto-oncogene PBF in thyroid cancer: a new target for augmenting radioiodine uptake.* The Journal of endocrinology, 2011. **210**(2): p. 157-63.
17. Read, M.L., et al., *Proto-oncogene PBF/PTTG1IP regulates thyroid cell growth and represses radioiodide treatment.* Cancer research, 2011. **71**(19): p. 6153-64.
18. Chien, W. and L. Pei, *A novel binding factor facilitates nuclear translocation and transcriptional activation function of the pituitary tumor-transforming gene product.* The Journal of biological chemistry, 2000. **275**(25): p. 19422-7.
19. Yaspo, M.L., et al., *Cloning of a novel human putative type Ia integral membrane protein mapping to 21q22.3.* Genomics, 1998. **49**(1): p. 133-6.
20. Watkins, R.J., et al., *Pituitary tumor transforming gene binding factor: a new gene in breast cancer.* Cancer research, 2010. **70**(9): p. 3739-49.

21. Stratford, A.L., et al., *Pituitary tumor transforming gene binding factor: a novel transforming gene in thyroid tumorigenesis.* The Journal of clinical endocrinology and metabolism, 2005. **90**(7): p. 4341-9.
22. Lau, N.C., et al., *An abundant class of tiny RNAs with probable regulatory roles in Caenorhabditis elegans.* Science, 2001. **294**(5543): p. 858-62.
23. Lagos-Quintana, M., et al., *Identification of novel genes coding for small expressed RNAs.* Science, 2001. **294**(5543): p. 853-8.
24. Mourelatos, Z., et al., *miRNPs: a novel class of ribonucleoproteins containing numerous microRNAs.* Genes & development, 2002. **16**(6): p. 720-8.
25. Lee, Y., et al., *MicroRNA genes are transcribed by RNA polymerase II.* The EMBO journal, 2004. **23**(20): p. 4051-60.
26. Cai, X., C.H. Hagedorn, and B.R. Cullen, *Human microRNAs are processed from capped, polyadenylated transcripts that can also function as mRNAs.* RNA, 2004. **10**(12): p. 1957-66.
27. Lee, Y., et al., *The nuclear RNase III Drosha initiates microRNA processing.* Nature, 2003. **425**(6956): p. 415-9.
28. Ketting, R.F., et al., *Dicer functions in RNA interference and in synthesis of small RNA involved in developmental timing in C. elegans.* Genes & development, 2001. **15**(20): p. 2654-9.
29. Bernstein, E., et al., *Role for a bidentate ribonuclease in the initiation step of RNA interference.* Nature, 2001. **409**(6818): p. 363-6.
30. Grishok, A., et al., *Genes and mechanisms related to RNA interference regulate expression of the small temporal RNAs that control C. elegans developmental timing.* Cell, 2001. **106**(1): p. 23-34.
31. Knight, S.W. and B.L. Bass, *A role for the RNase III enzyme DCR-1 in RNA interference and germ line development in Caenorhabditis elegans.* Science, 2001. **293**(5538): p. 2269-71.
32. Kim, V.N., *MicroRNA biogenesis: coordinated cropping and dicing.* Nature reviews. Molecular cell biology, 2005. **6**(5): p. 376-85.
33. Jones-Rhoades, M.W. and D.P. Bartel, *Computational identification of plant microRNAs and their targets, including a stress-induced miRNA.* Molecular cell, 2004. **14**(6): p. 787-99.
34. Bartel, D.P., *MicroRNAs: genomics, biogenesis, mechanism, and function.* Cell, 2004. **116**(2): p. 281-97.
35. Pallante, P., et al., *MicroRNA deregulation in human thyroid papillary carcinomas.* Endocrine-related cancer, 2006. **13**(2): p. 497-508.
36. Liu, C.G., et al., *An oligonucleotide microchip for genome-wide microRNA profiling in human and mouse tissues.* Proceedings of the National Academy of Sciences of the United States of America, 2004. **101**(26): p. 9740-4.
37. Sempere, L.F., et al., *Expression profiling of mammalian microRNAs uncovers a subset of brain-expressed microRNAs with possible roles in murine and human neuronal differentiation.* Genome biology, 2004. **5**(3): p. R13.
38. Tuschl, T., et al., *Targeted mRNA degradation by double-stranded RNA in vitro.* Genes & development, 1999. **13**(24): p. 3191-7.
39. Hammond, S.M., et al., *An RNA-directed nuclease mediates post-transcriptional gene silencing in Drosophila cells.* Nature, 2000. **404**(6775): p. 293-6.
40. Llave, C., et al., *Endogenous and silencing-associated small RNAs in plants.* The Plant cell, 2002. **14**(7): p. 1605-19.
41. Valencia-Sanchez, M.A., et al., *Control of translation and mRNA degradation by miRNAs and siRNAs.* Genes & development, 2006. **20**(5): p. 515-24.
42. Lee, R.C., R.L. Feinbaum, and V. Ambros, *The C. elegans heterochronic gene lin-4 encodes small RNAs with antisense complementarity to lin-14.* Cell, 1993. **75**(5): p. 843-54.
43. Wightman, B., I. Ha, and G. Ruvkun, *Posttranscriptional regulation of the heterochronic gene lin-14 by lin-4 mediates temporal pattern formation in C. elegans.* Cell, 1993. **75**(5): p. 855-62.
44. Liu, J., et al., *Argonaute2 is the catalytic engine of mammalian RNAi.* Science, 2004. **305**(5689): p. 1437-41.

45. Sen, G.L. and H.M. Blau, *Argonaute 2/RISC resides in sites of mammalian mRNA decay known as cytoplasmic bodies.* Nature cell biology, 2005. **7**(6): p. 633-6.
46. Pillai, R.S., et al., *Inhibition of translational initiation by Let-7 MicroRNA in human cells.* Science, 2005. **309**(5740): p. 1573-6.
47. Brennecke, J., et al., *bantam encodes a developmentally regulated microRNA that controls cell proliferation and regulates the proapoptotic gene hid in Drosophila.* Cell, 2003. **113**(1): p. 25-36.
48. Poy, M.N., et al., *A pancreatic islet-specific microRNA regulates insulin secretion.* Nature, 2004. **432**(7014): p. 226-30.
49. Thai, T.H., et al., *Regulation of the germinal center response by microRNA-155.* Science, 2007. **316**(5824): p. 604-8.
50. Bushati, N. and S.M. Cohen, *microRNA functions.* Annual review of cell and developmental biology, 2007. **23**: p. 175-205.
51. Nie, J., et al., *microRNA-365, down-regulated in colon cancer, inhibits cell cycle progression and promotes apoptosis of colon cancer cells by probably targeting Cyclin D1 and Bcl-2.* Carcinogenesis, 2012. **33**(1): p. 220-5.
52. Liang, Y.J., et al., *MiR-124 targets Slug to regulate epithelial-mesenchymal transition and metastasis of breast cancer.* Carcinogenesis, 2013. **34**(3): p. 713-22.
53. He, H., et al., *The role of microRNA genes in papillary thyroid carcinoma.* Proceedings of the National Academy of Sciences of the United States of America, 2005. **102**(52): p. 19075-80.
54. Nikiforova, M.N., et al., *MicroRNA expression profiling of thyroid tumors: biological significance and diagnostic utility.* The Journal of clinical endocrinology and metabolism, 2008. **93**(5): p. 1600-8.
55. Nikiforova, M.N. and Y.E. Nikiforov, *Molecular genetics of thyroid cancer: implications for diagnosis, treatment and prognosis.* Expert review of molecular diagnostics, 2008. **8**(1): p. 83-95.
56. Chen, Y.T., et al., *MicroRNA analysis as a potential diagnostic tool for papillary thyroid carcinoma.* Modern pathology : an official journal of the United States and Canadian Academy of Pathology, Inc, 2008. **21**(9): p. 1139-46.
57. Yip, L., et al., *MicroRNA signature distinguishes the degree of aggressiveness of papillary thyroid carcinoma.* Annals of surgical oncology, 2011. **18**(7): p. 2035-41.
58. Jazdzewski, K., et al., *Thyroid hormone receptor beta (THRB) is a major target gene for microRNAs deregulated in papillary thyroid carcinoma (PTC).* The Journal of clinical endocrinology and metabolism, 2011. **96**(3): p. E546-53.
59. Li, C., et al., *Hepatitis B virus mRNA-mediated miR-122 inhibition upregulates PTTG1-binding protein, which promotes hepatocellular carcinoma tumor growth and cell invasion.* Journal of virology, 2013. **87**(4): p. 2193-205.
60. Huang, T.H., et al., *MiRFinder: an improved approach and software implementation for genome-wide fast microRNA precursor scans.* BMC bioinformatics, 2007. **8**: p. 341.
61. Min, H. and S. Yoon, *Got target? Computational methods for microRNA target prediction and their extension.* Experimental & molecular medicine, 2010. **42**(4): p. 233-44.
62. Lewis, B.P., et al., *Prediction of mammalian microRNA targets.* Cell, 2003. **115**(7): p. 787-98.
63. Lee, M.R., J.S. Kim, and K.S. Kim, *miR-124a is important for migratory cell fate transition during gastrulation of human embryonic stem cells.* Stem cells, 2010. **28**(9): p. 1550-9.
64. Furuta, M., et al., *miR-124 and miR-203 are epigenetically silenced tumor-suppressive microRNAs in hepatocellular carcinoma.* Carcinogenesis, 2010. **31**(5): p. 766-76.
65. Hunt, S., et al., *MicroRNA-124 suppresses oral squamous cell carcinoma motility by targeting ITGB1.* FEBS letters, 2011. **585**(1): p. 187-92.
66. Xia, H., et al., *Loss of brain-enriched miR-124 microRNA enhances stem-like traits and invasiveness of glioma cells.* The Journal of biological chemistry, 2012. **287**(13): p. 9962-71.
67. Lim, L.P., et al., *Microarray analysis shows that some microRNAs downregulate large numbers of target mRNAs.* Nature, 2005. **433**(7027): p. 769-73.

68. Maes, O.C., H. Sarojini, and E. Wang, *Stepwise up-regulation of microRNA expression levels from replicating to reversible and irreversible growth arrest states in WI-38 human fibroblasts.* Journal of cellular physiology, 2009. **221**(1): p. 109-19.
69. Streicher, K.L., et al., *A novel oncogenic role for the miRNA-506-514 cluster in initiating melanocyte transformation and promoting melanoma growth.* Oncogene, 2012. **31**(12): p. 1558-70.
70. Long, Q., et al., *Protein-coding and microRNA biomarkers of recurrence of prostate cancer following radical prostatectomy.* The American journal of pathology, 2011. **179**(1): p. 46-54.
71. Taylor, D.D. and C. Gercel-Taylor, *MicroRNA signatures of tumor-derived exosomes as diagnostic biomarkers of ovarian cancer.* Gynecologic oncology, 2008. **110**(1): p. 13-21.
72. Smith, V., et al., *Manipulation of PBF/PTTG1IP phosphorylation status; a potential new therapeutic strategy for improving radioiodine uptake in thyroid and other tumors.* The Journal of clinical endocrinology and metabolism, 2013.
73. Boelaert, K., et al., *PTTG and PBF repress the human sodium iodide symporter.* Oncogene, 2007. **26**(30): p. 4344-56.
74. Alexiou, P., et al., *Lost in translation: an assessment and perspective for computational microRNA target identification.* Bioinformatics, 2009. **25**(23): p. 3049-55.
75. Bandres, E., et al., *Identification by Real-time PCR of 13 mature microRNAs differentially expressed in colorectal cancer and non-tumoral tissues.* Molecular cancer, 2006. **5**: p. 29.